Optimizing Piezoelectric Stack Preload Bolts in Ultrasonic Transducers

Dominick A. DeAngelis, Gary W. Schulze and K.S. Wong

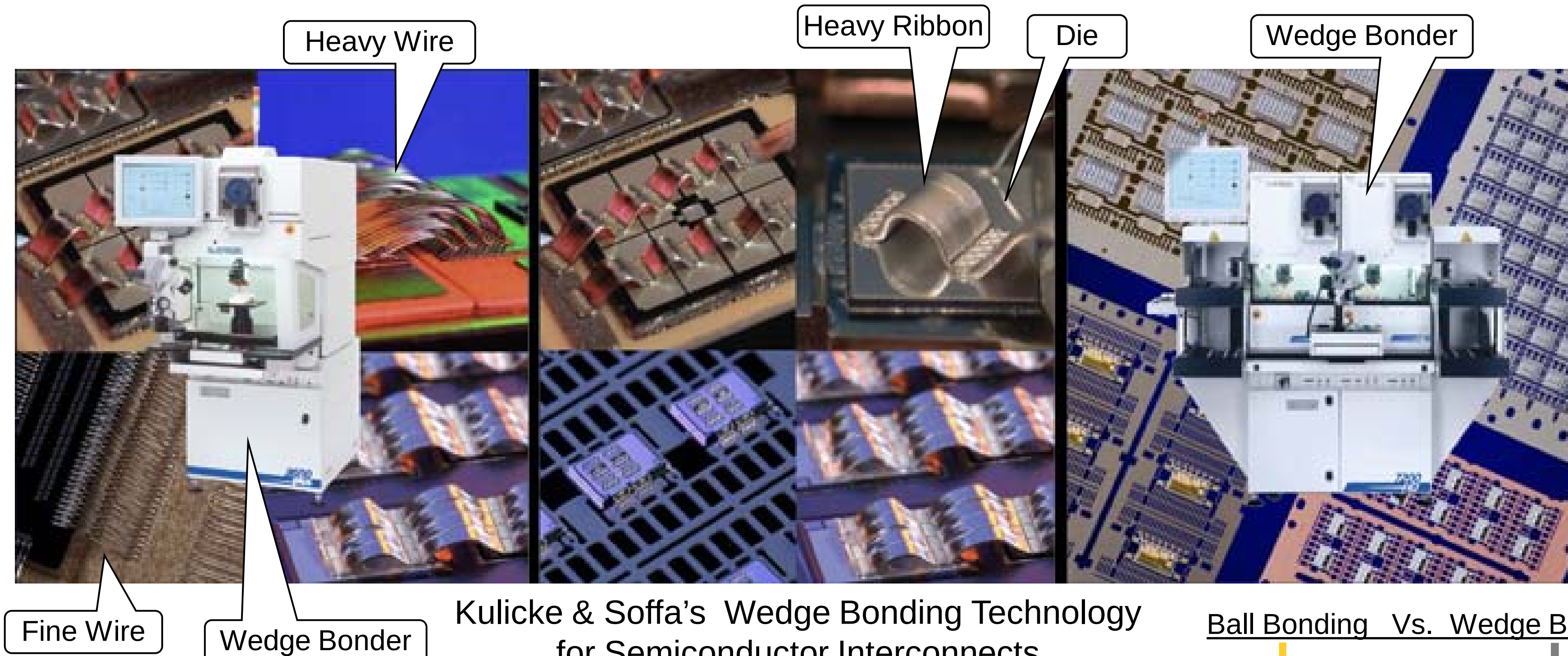

Kulicke & Soffa's Wedge Bonding Technology for Semiconductor Interconnects

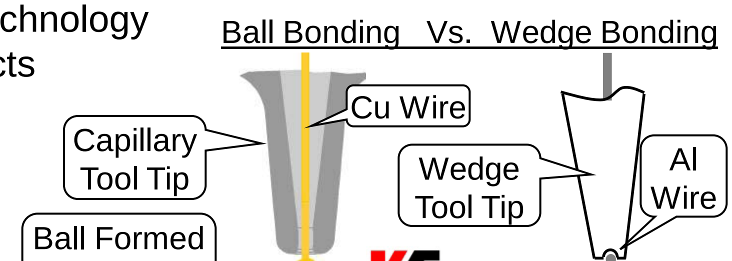

OUTLINE

- Langevin Type “Sandwich” Transducers Used in Wire Bonding
- Motivation for the Research
- Pros and Cons of Common Piezo Stack Preload Bolt Configurations
- Common Transducer Failure Modes Caused by Preload Bolts
- Selection of Bolt Material Based on Strength and E-Mech Coupling
- Sizing of Preload Bolts Based on Prestress Uniformity and Yield Stress
- Determining Minimum Thread Engagement to the Mating Horn
- First Pass (Non FEA) Prediction of Parasitic Bolt Resonances
- Conclusions
- Questions?

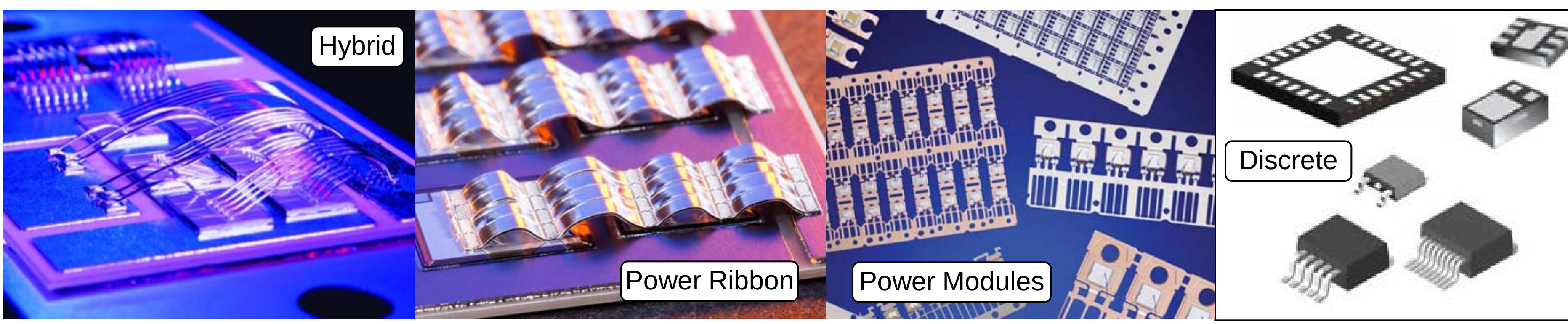

TRANSDUCERS FOR WIRE BONDING

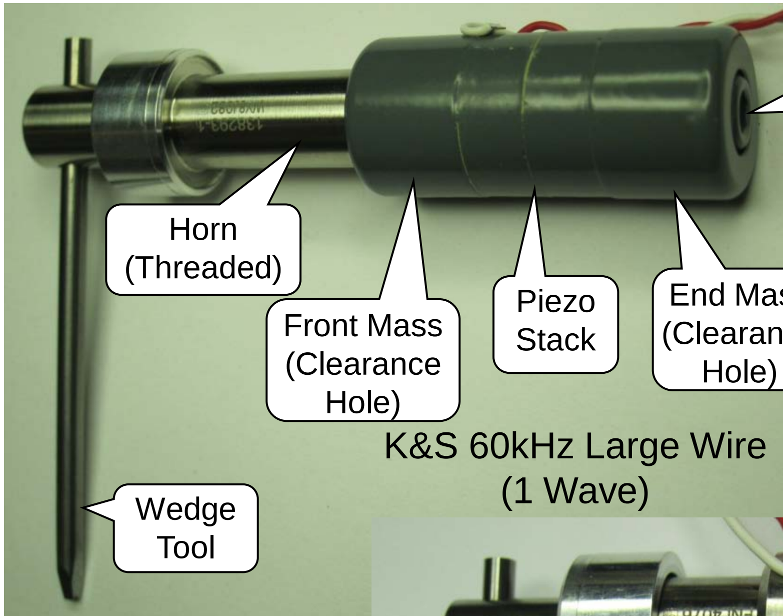

K&S 60kHz Large Wire (1 Wave)

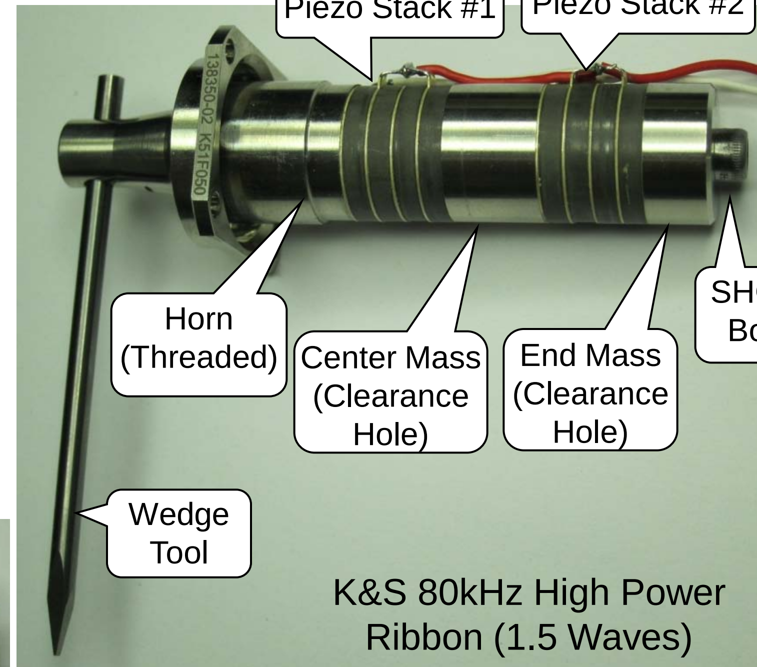

K&S 80kHz High Power Ribbon (1.5 Waves)

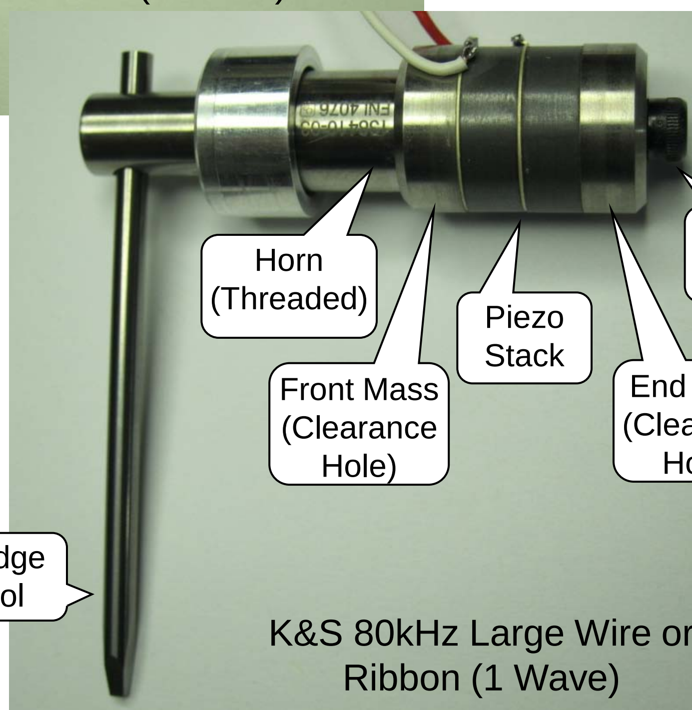

K&S 80kHz Large Wire or Ribbon (1 Wave)

All Piezo Rings Have Clearance Hole for Preload Bolt

TRANSDUCERS FOR WIRE BONDING

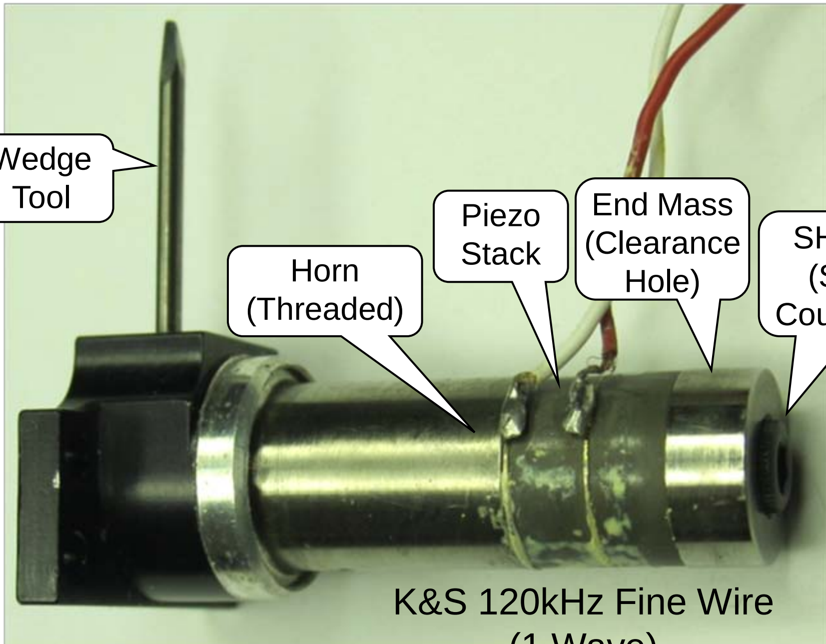

K&S 120kHz Fine Wire (1 Wave)

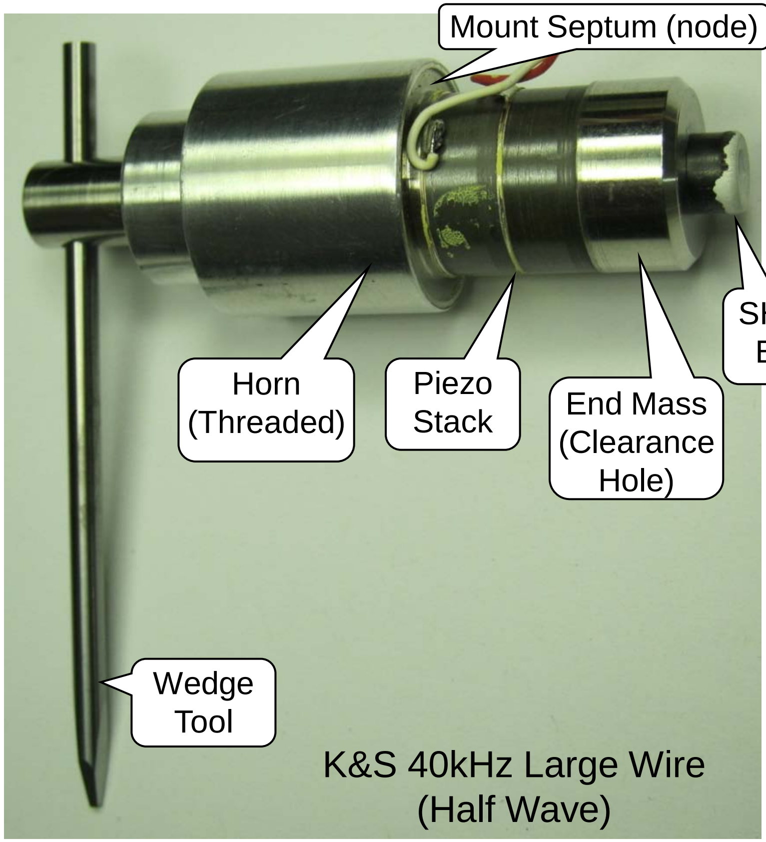

K&S 40kHz Large Wire (Half Wave)

All Piezo Rings Have Clearance Hole for Preload Bolt

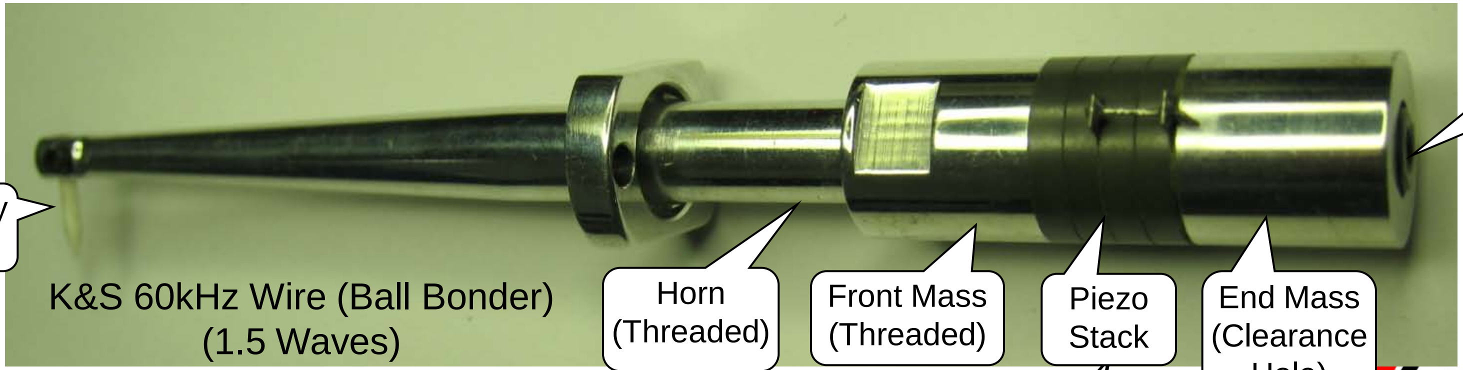

K&S 60kHz Wire (Ball Bonder) (1.5 Waves)

MOTIVATION FOR THE RESEARCH

- Selection of the preload bolt is often an afterthought in the design of Langevin type "sandwich" transducers
- Even within transducer design companies (such as K&S), there is no consistent methodology for design or configuration of preload bolts
- Quite often the preload bolt is the root cause of failure for power ultrasonic transducers (yield/breakage, preload loss, parasitic mode…)
- Main role of preload bolt is to provide a "prestress" in the piezo stack to prevent interface "gapping" or tension in glue joints (delamination)
- Preload bolts are an <u>integral part</u> of the highly tuned dynamic system
- Resulting parasitic resonances in preload bolts such as bending or longitudinal modes are often difficult to predict and control
- Some rule-of-thumb design and configuration guidelines for preload bolts are needed

COMMON PRELOAD BOLT CONFIG'S

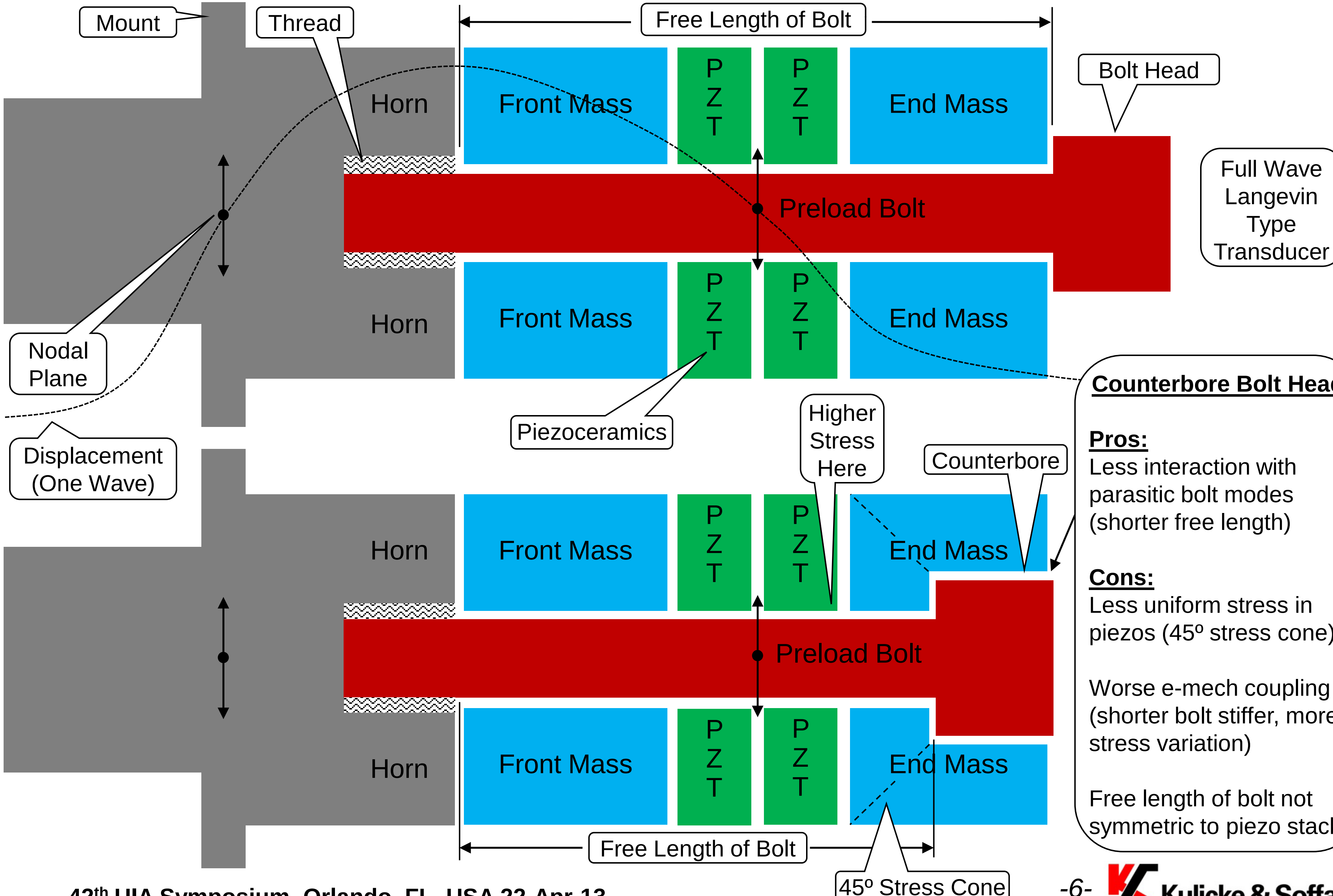

Counterbore Bolt Head

Pros:
Less interaction with parasitic bolt modes (shorter free length)

Cons:
Less uniform stress in piezos (45º stress cone)

Worse e-mech coupling (shorter bolt stiffer, more stress variation)

Free length of bolt not symmetric to piezo stack

COMMON PRELOAD BOLT CONFIG'S

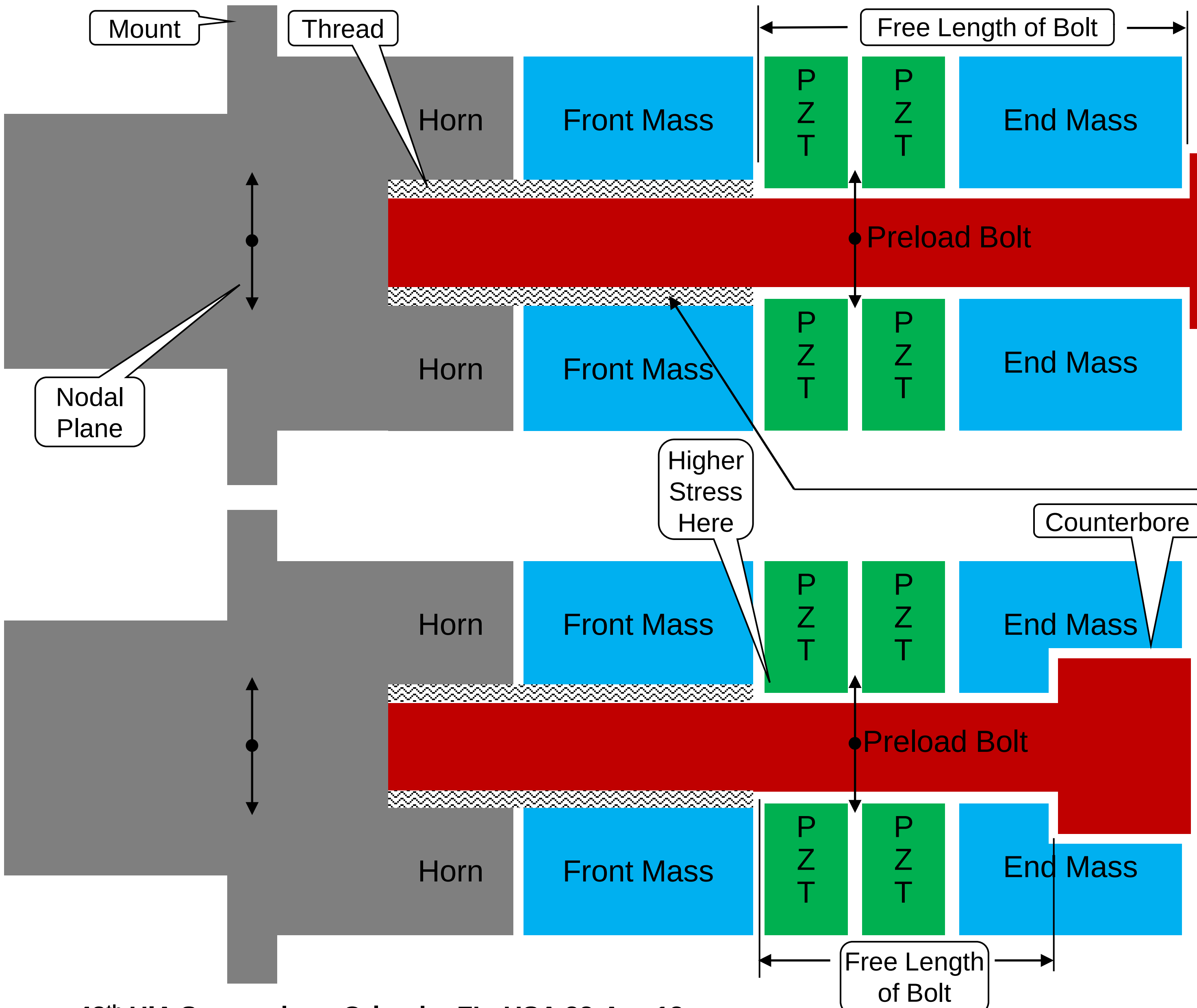

Threaded Front Mass

Pros:
Less interaction with parasitic bolt modes (shorter free length)

Cons:
Less uniform stress in piezos (thread on PZT)

Worse e-mech coupling (shorter bolt stiffer, more stress variation)

Free length of bolt not symmetric to piezo stack

COMMON PRELOAD BOLT CONFIG'S

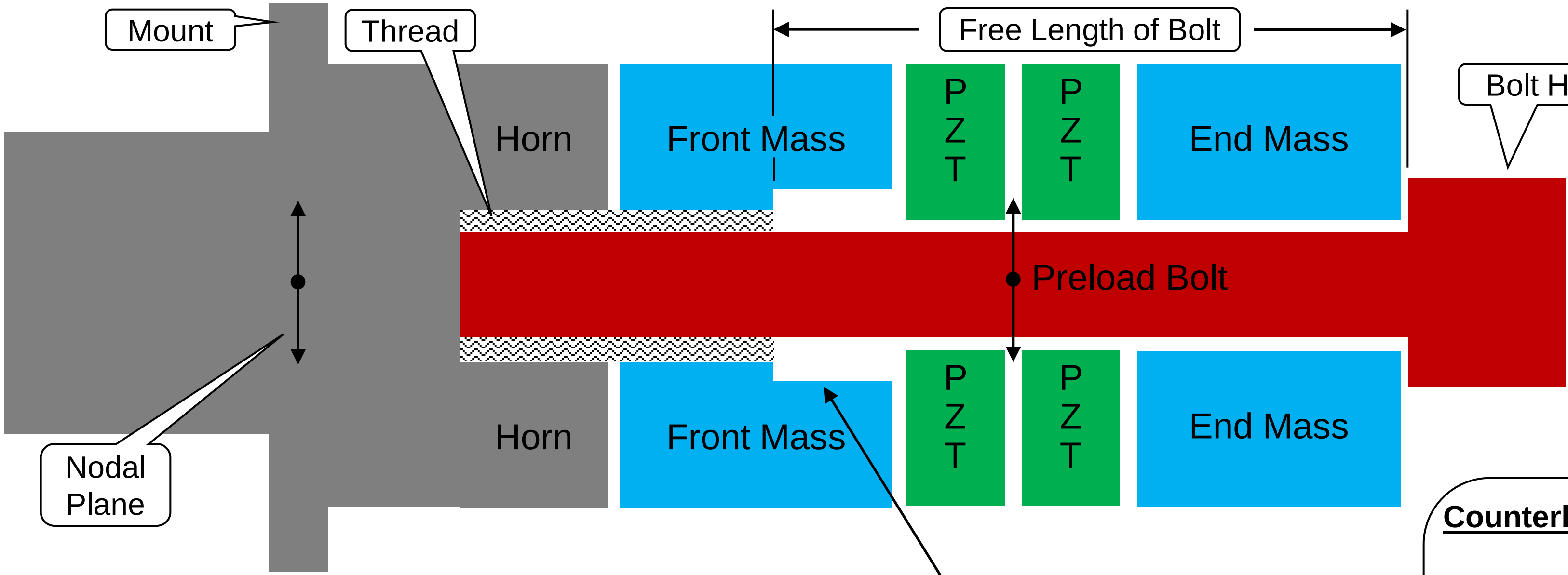

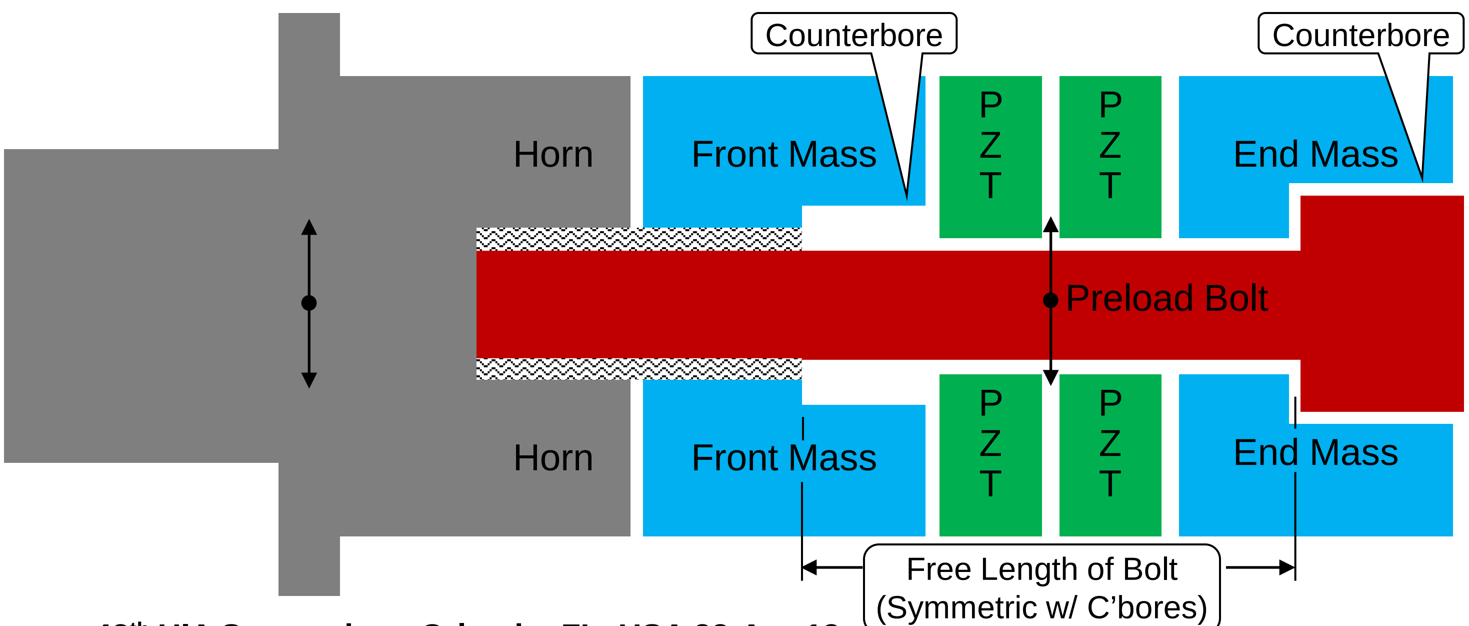

Counterbore Front Mass

Pros:

More uniform stress in piezos

Better e-mech (k) coupling (longer bolt less stiff, uniform stress)

Cons:

More interaction with parasitic bolt modes (longer free length of bolt)

Free length of bolt not symmetric to piezo stack

COMMON PRELOAD BOLT CONFIG'S

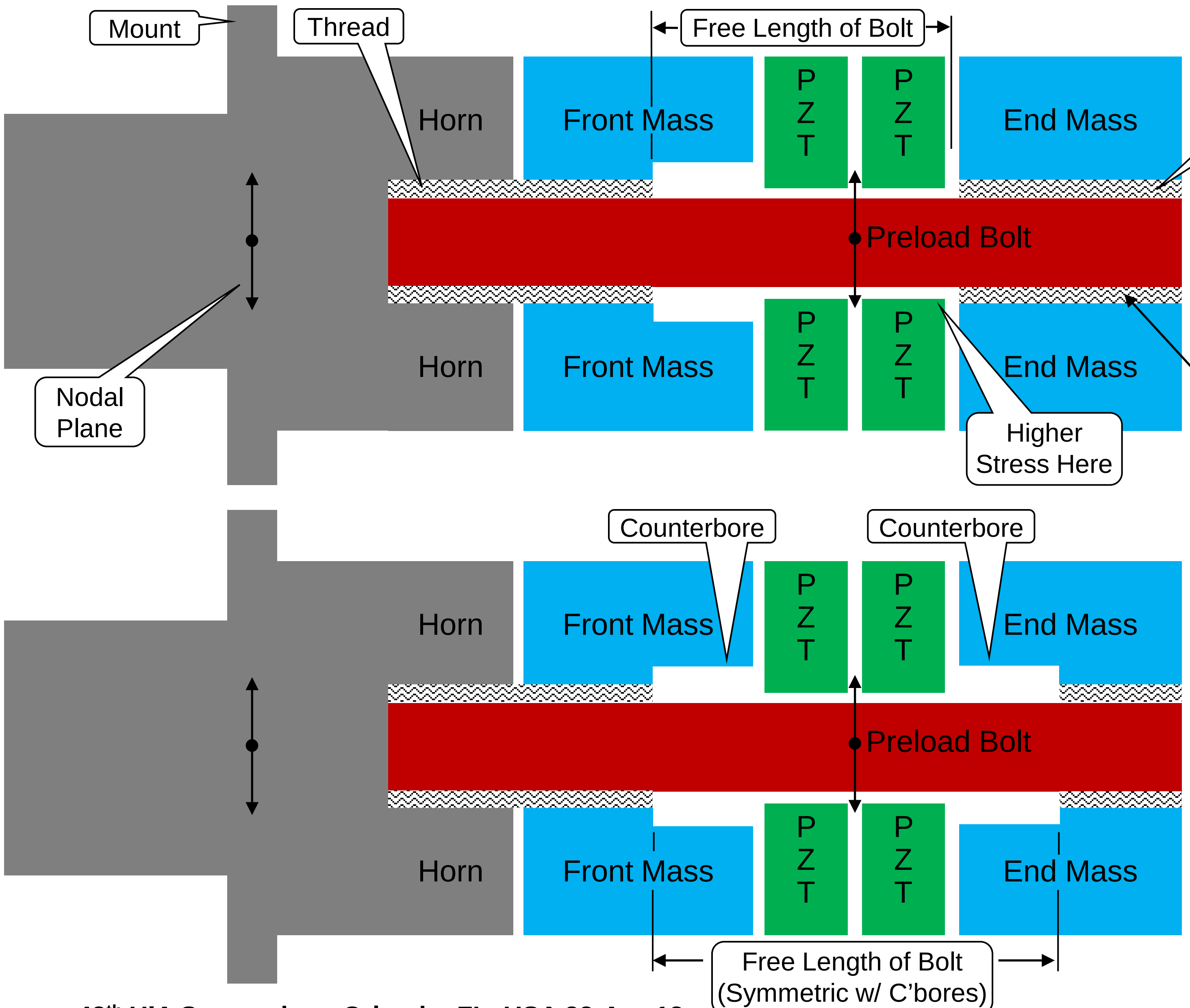

<u>Threaded End Mass</u>

<u>Pros:</u>
Less interaction with parasitic bolt modes (shorter free length)

<u>Cons:</u>
Less uniform stress in piezos

Worse elec-mech (k) coupling (shorter bolt stiffer, stress variation)

Free length of bolt not symmetric to piezo stack

Rotational rubbing against piezos with assembly

COMMON PRELOAD BOLT CONFIG'S

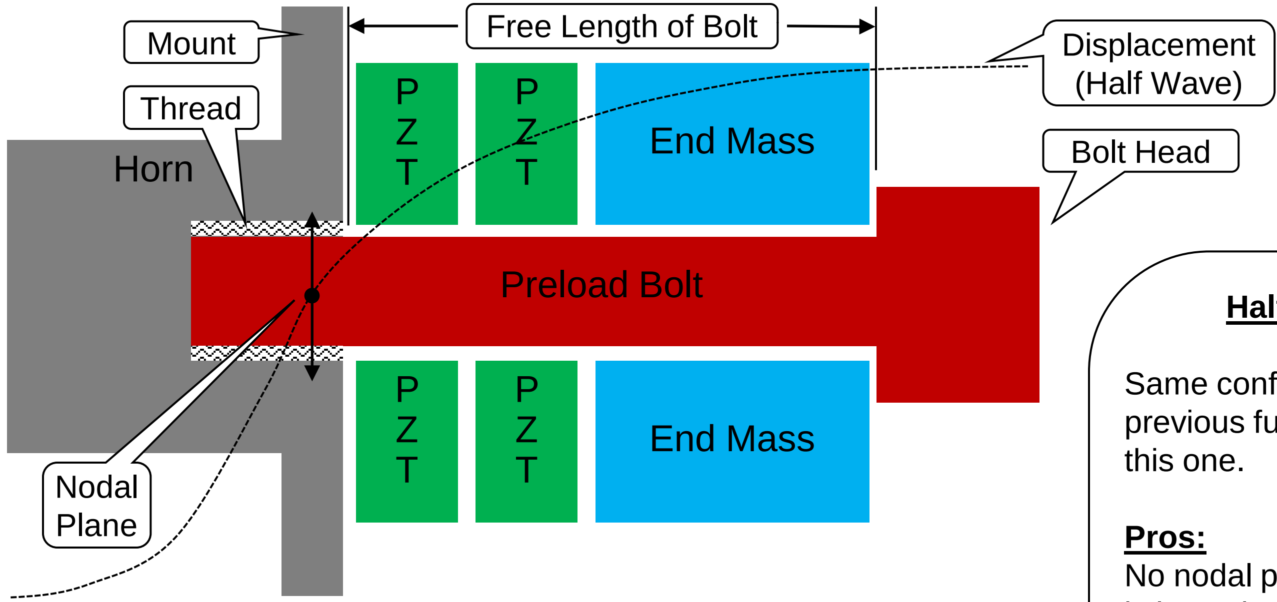

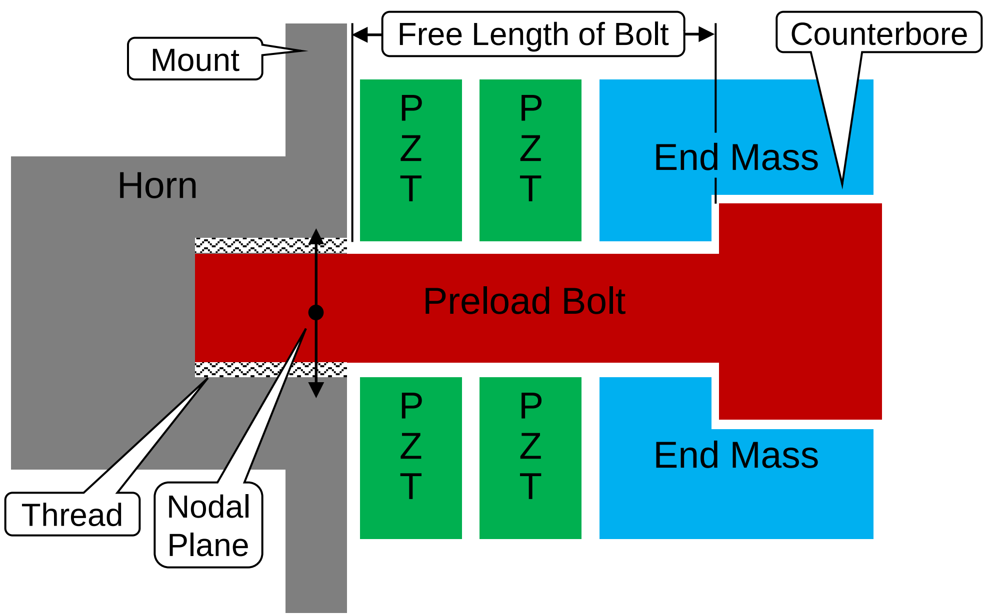

<u>Half Wave Transducer Design</u>

Same configurations with pros/cons from previous full wave transducers also apply to this one.

<u>Pros:</u>

No nodal planes in piezos so operating stress is lower in PZT (piezo material usually has lowest strength) and current gain is higher

Smaller transducer size for lower frequencies

<u>Cons:</u>

Threaded regions lie in nodal plane where highest stress occurs

No nodal planes in piezos so driver is less efficient (higher impedance, lower e-mech coupling)

Typical Laser Vibrometer Data for Known Good 80kHz Transducer

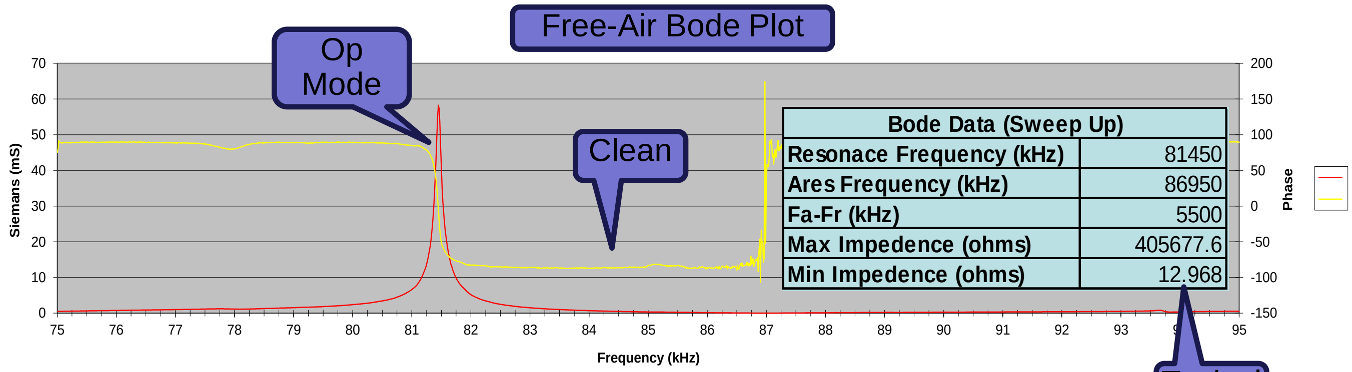

Bode Data (Sweep Up)	
Resonace Frequency (kHz)	81450
Ares Frequency (kHz)	86950
Fa-Fr (kHz)	5500
Max Impedence (ohms)	405677.6
Min Impedence (ohms)	12.968

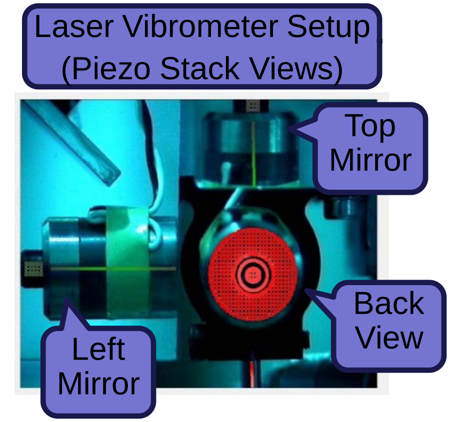

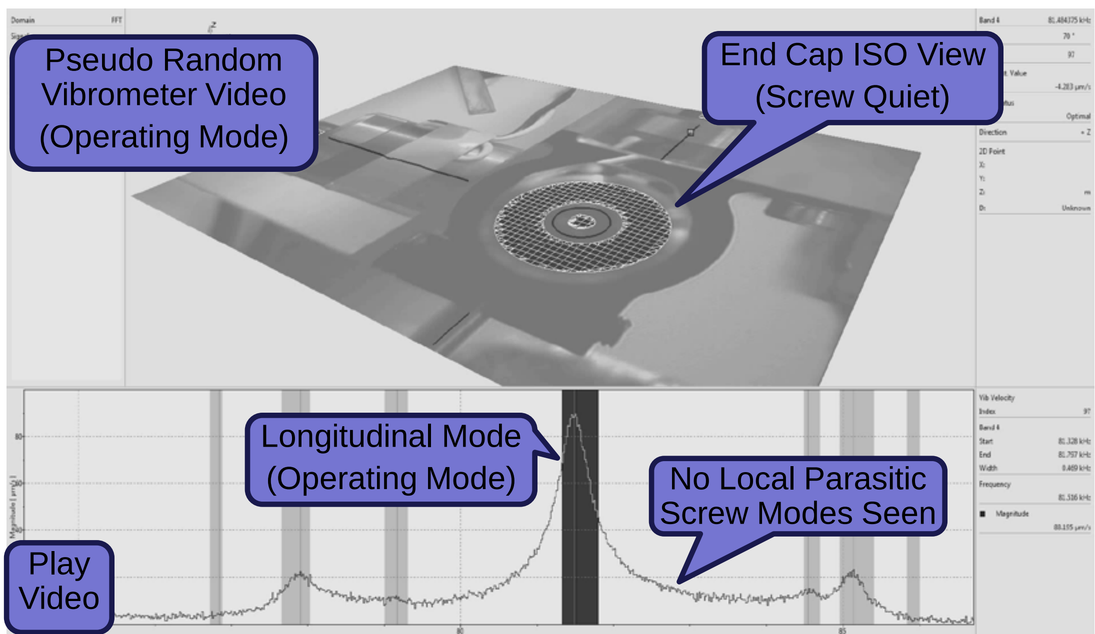

Observations

- Preload screw is fairly well behaved at operating mode
- No parasitic resonances in the preload screw near operating mode for this transducer
- Location of parasitic screw modes can be inconsistent with glued piezo stack designs

FAILURE MODES OF PRELOAD BOLTS

Data for Failed 80kHz Transducer with Longitudinal Screw Resonance

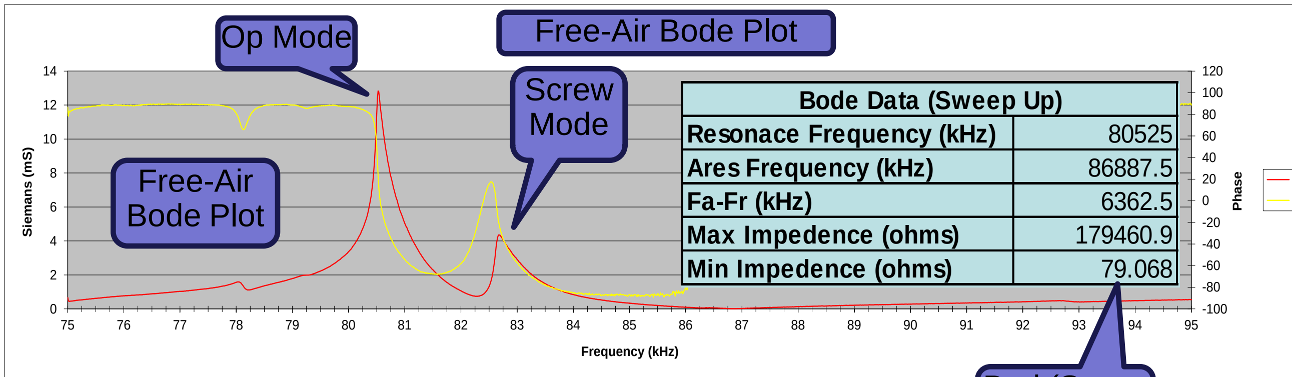

Bode Data (Sweep Up)	
Resonace Frequency (kHz)	80525
Ares Frequency (kHz)	86887.5
Fa-Fr (kHz)	6362.5
Max Impedence (ohms)	179460.9
Min Impedence (ohms)	79.068

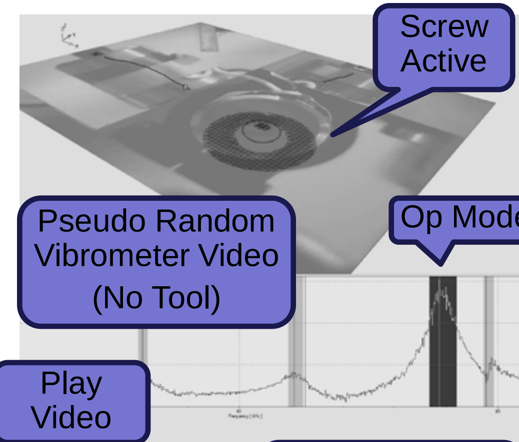

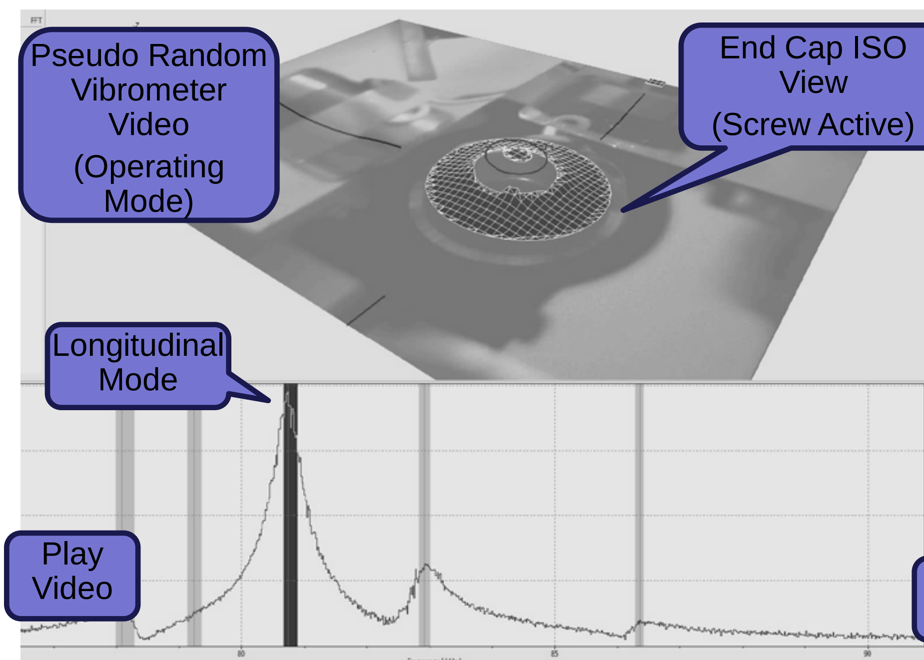

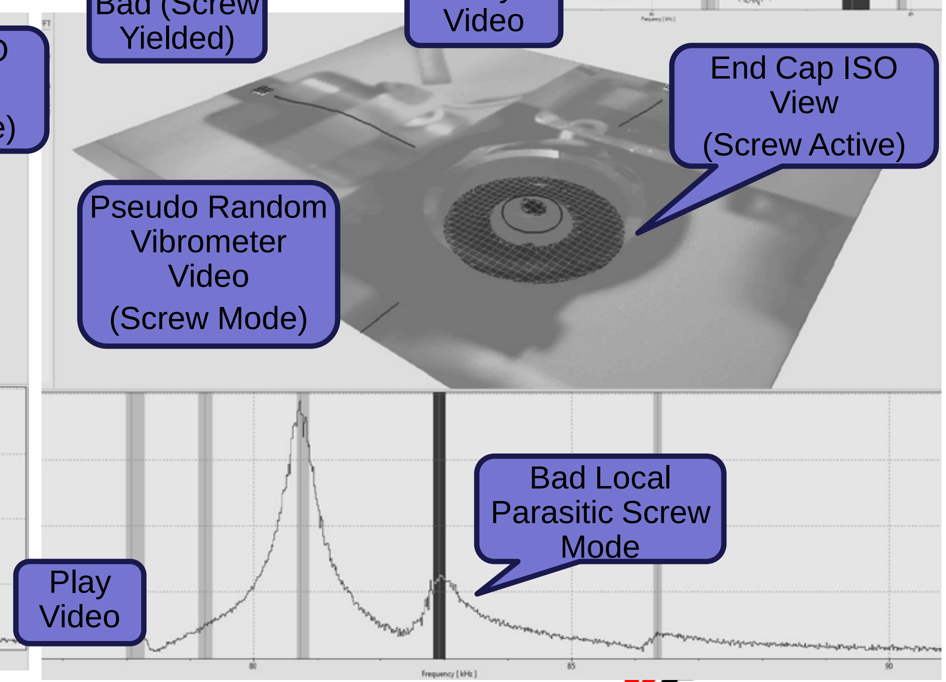

Data for Failed 80kHz Transducer with Bending Screw Resonance

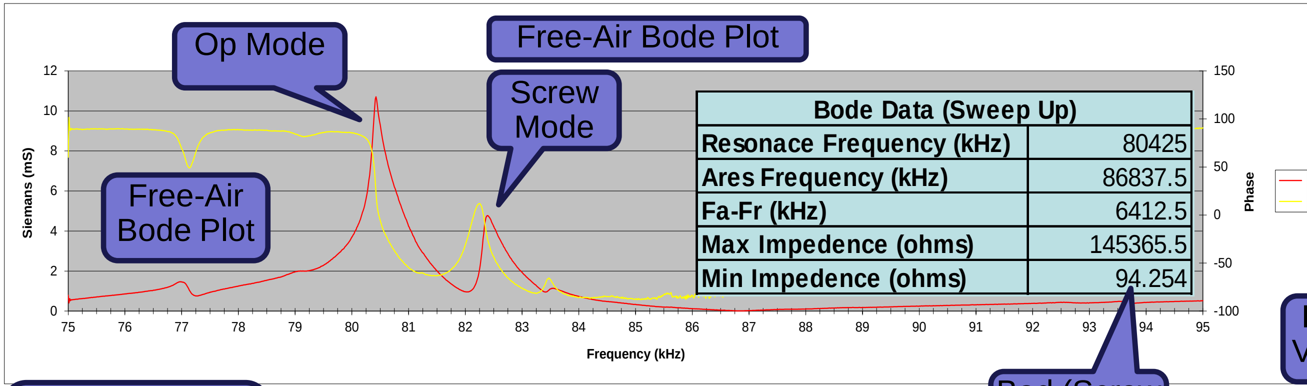

Bode Data (Sweep Up)	
Resonace Frequency (kHz)	80425
Ares Frequency (kHz)	86837.5
Fa-Fr (kHz)	6412.5
Max Impedence (ohms)	145365.5
Min Impedence (ohms)	94.254

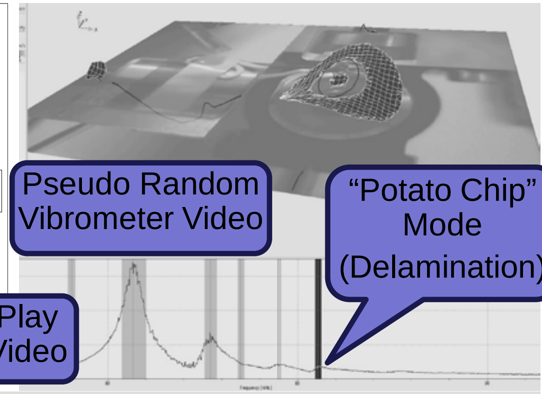

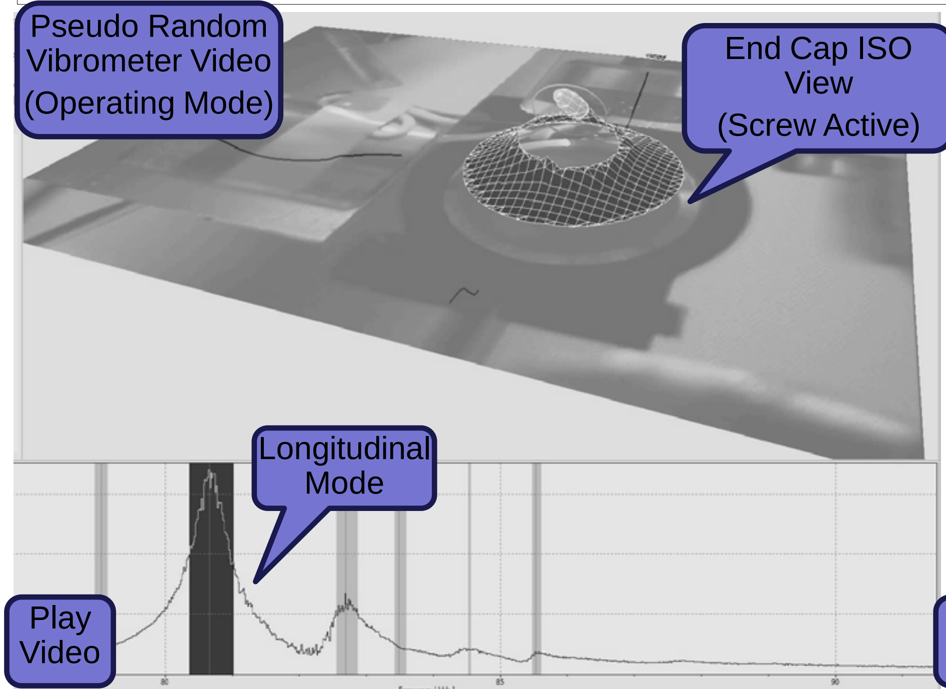

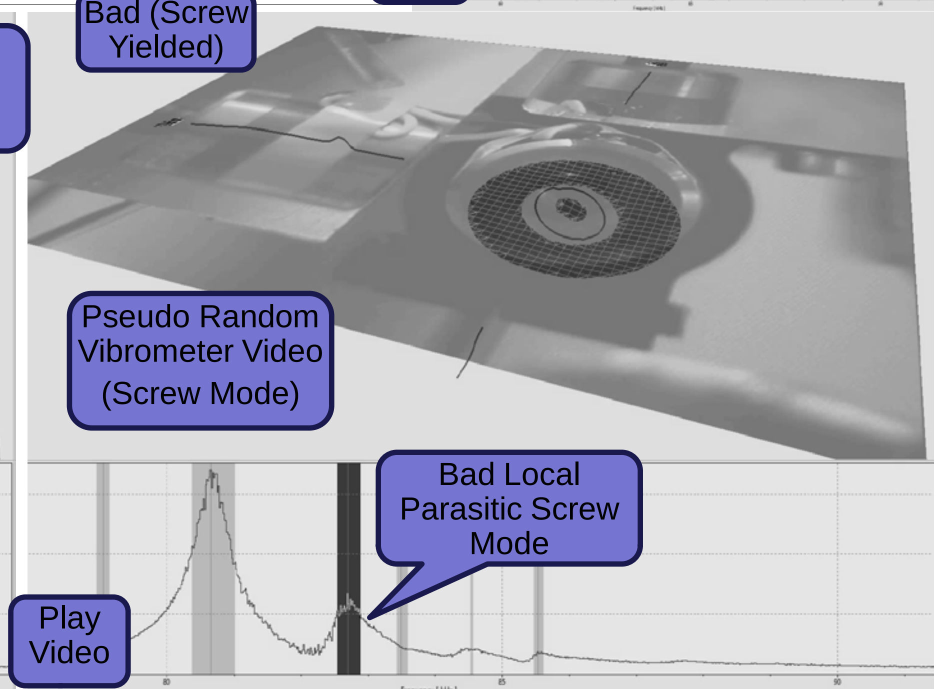

FAILURE MODES OF PRELOAD BOLTS

Example: Transducer – Preload Screw Resonance Analysis

Comparison of laser vibrometer and finite element evaluation of K&S 80kHz transducer

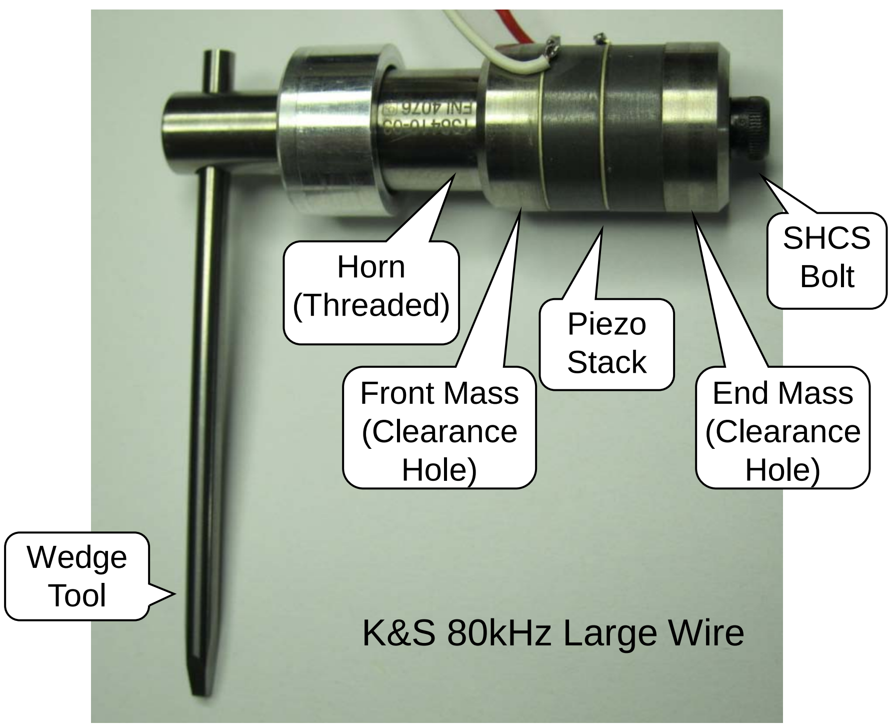

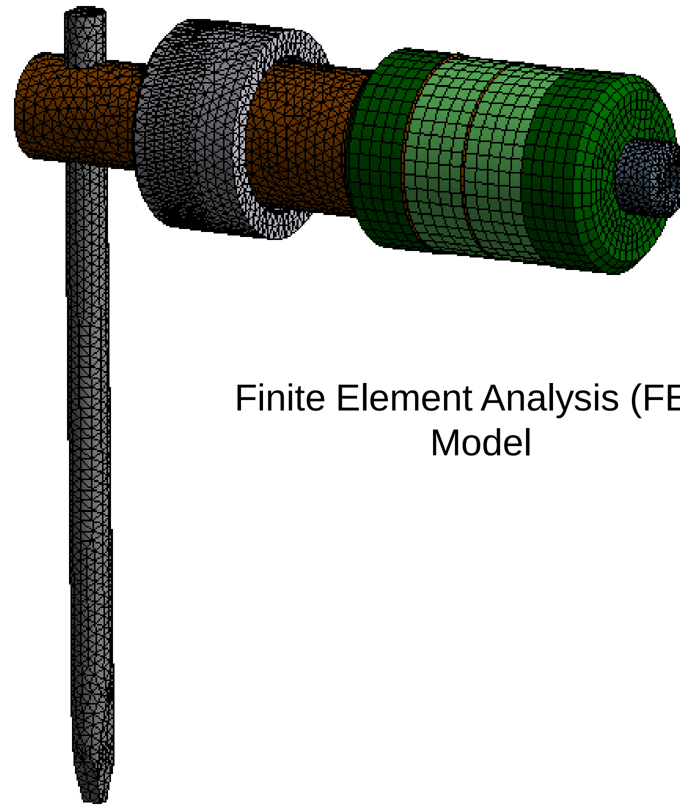

Finite Element Analysis (FEA) Model

Example: Transducer – Preload Screw Resonance Analysis

<u>Known good transducer (operating mode)</u>

- No nearby parasitic modes seen
- Stable, low impedance
- Boundary conditions on screw modeled with full contact area under head

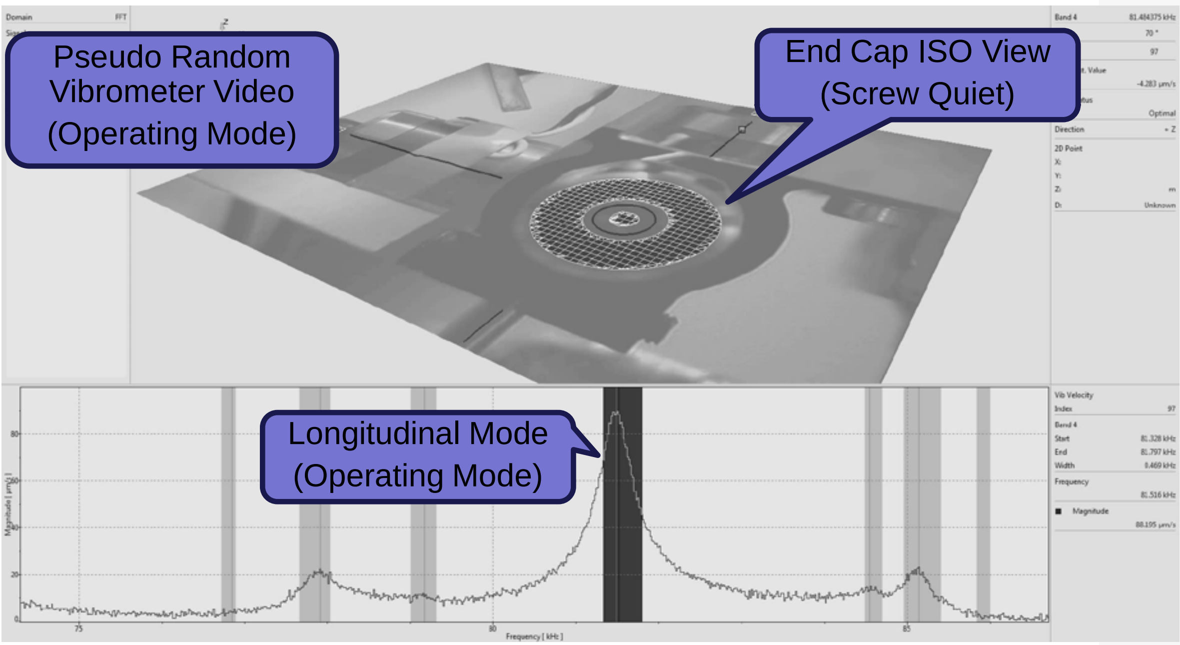

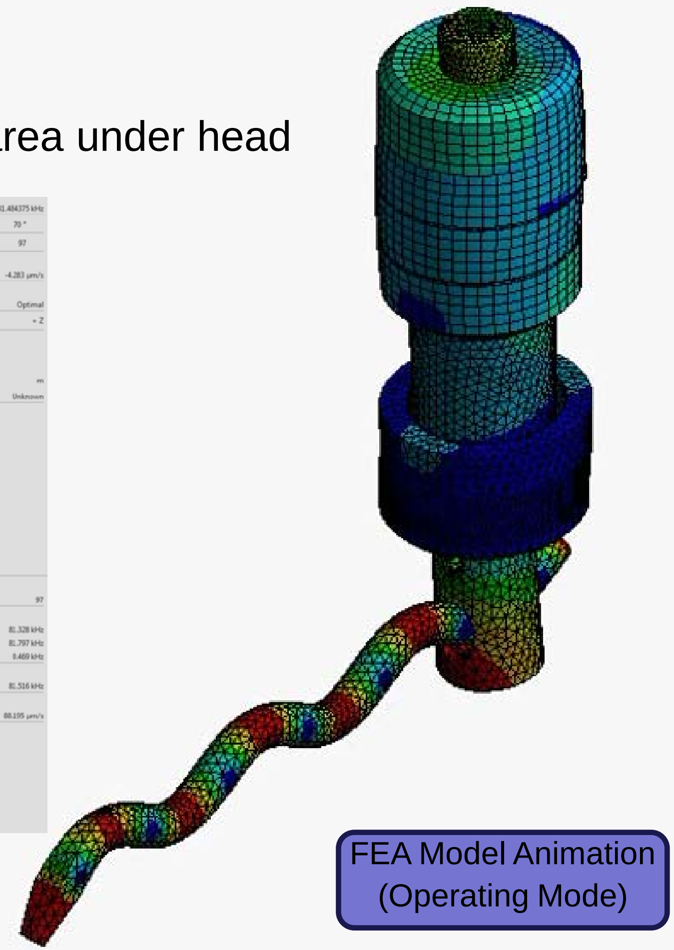

Play Video

Example: Transducer – Preload Screw Resonance Analysis

Known bad transducer (operating mode)

- Low preload due to screw yielding (modeled as reduced contact area with screw)
- Nearby parasitic mode
- Unstable, high impedance

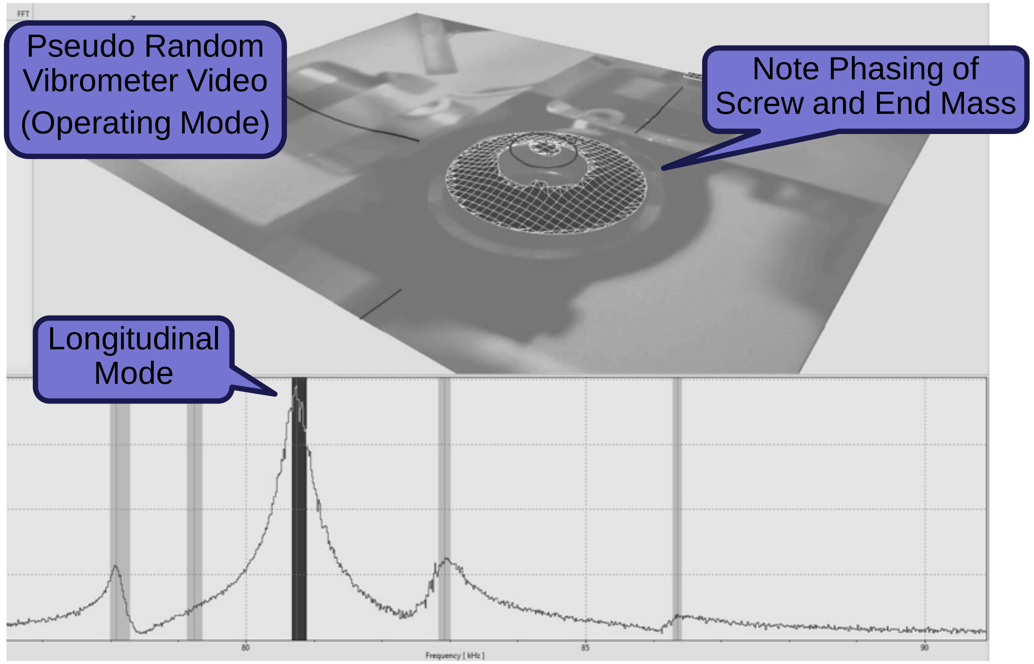

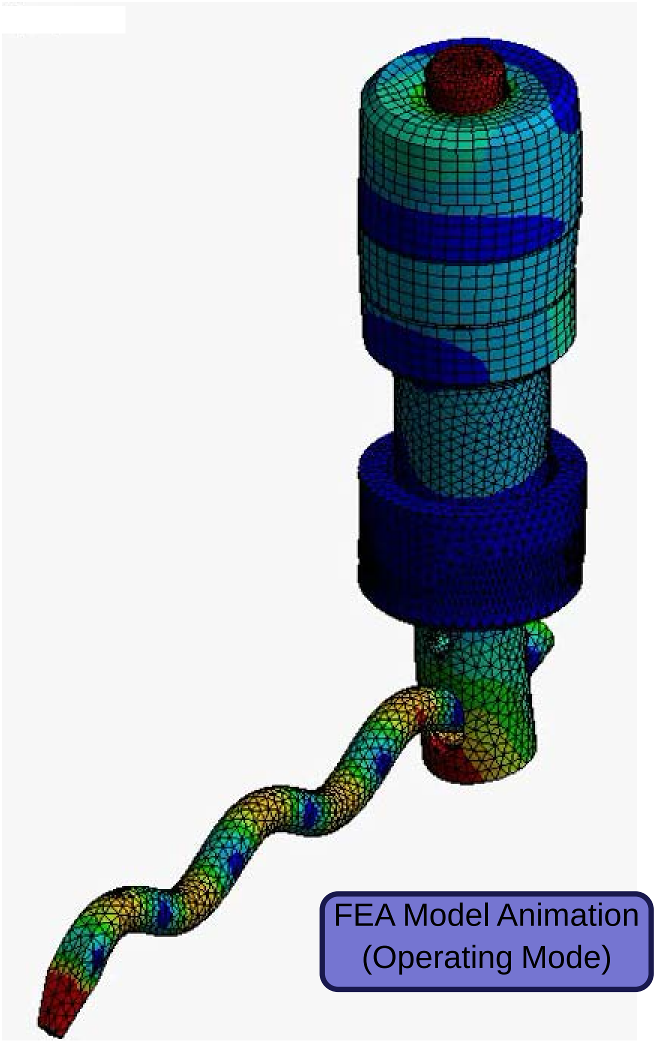

Play Video

Example: Transducer – Preload Screw Resonance Analysis

<u>Known bad transducer (longitudinal screw mode)</u>

- Low preload due to screw yielding (FEA modeled as reduced contact area under screw head)
- Nearby parasitic mode
- Unstable, high impedance

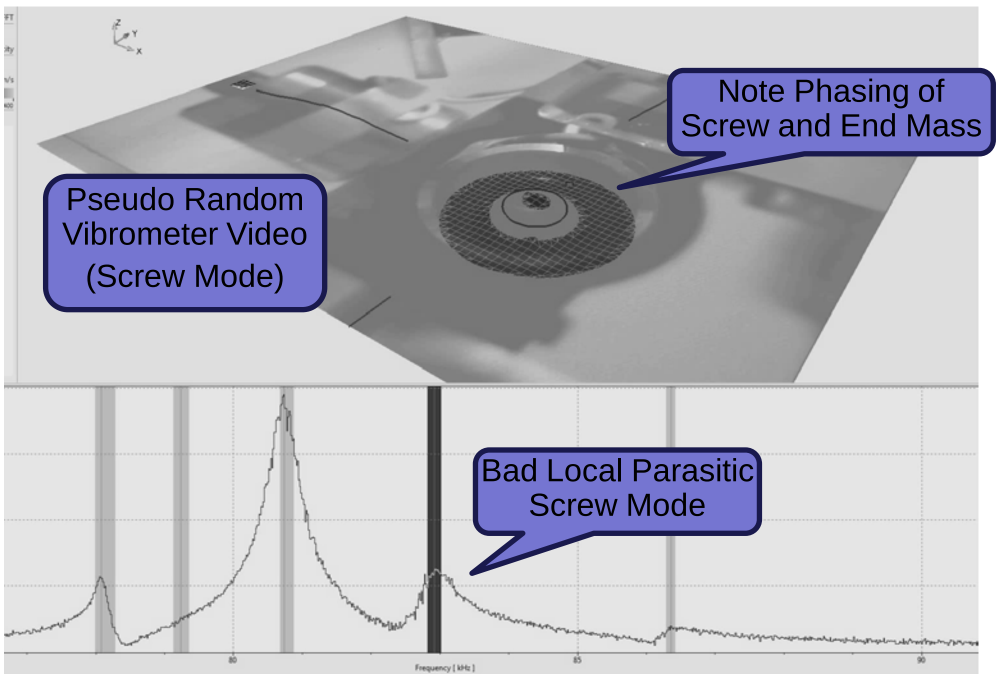

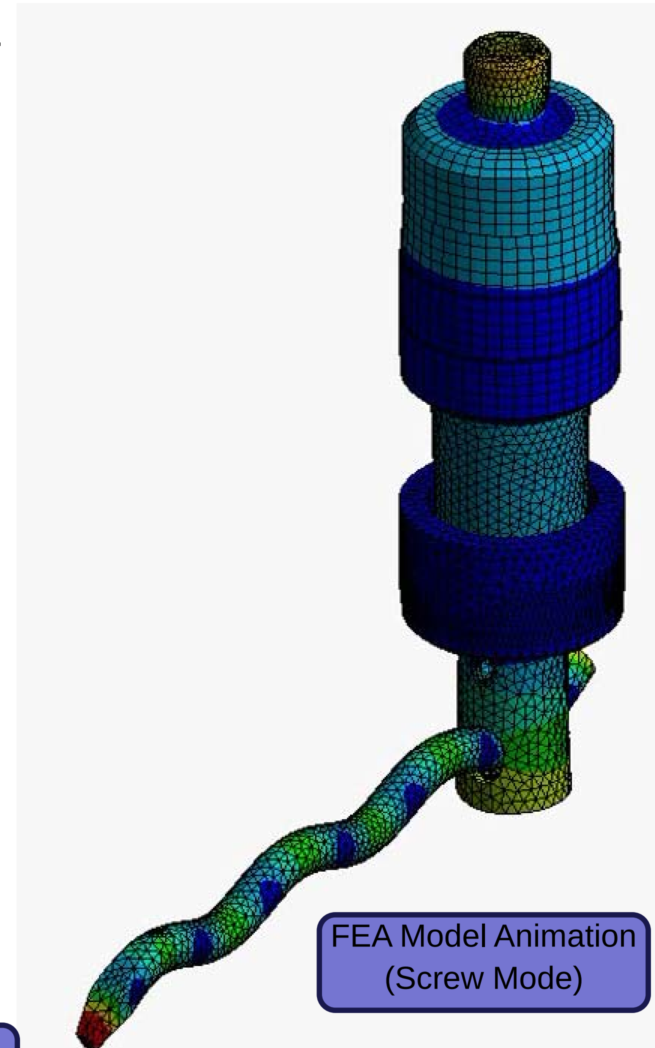

Play Video

FAILURE MODES OF PRELOAD BOLTS

Example: Transducer – Preload Screw Resonance Analysis

<u>Closer look via section views: What is the motion of the screw?</u>

- The screw resonance mode here may be described as “slinky-like” (i.e., longitudinal mode)
- Screw mode has “one end” out of phase with the natural driver motion
- This situation has the potential to exert very high loads at preload screw threads
- Alternate axis-symmetric FEA models would have predicted this slinky mode, but will have missed all the bending modes in screw (common mistake)

Screw Resonance Mode

Transducer Operating Mode

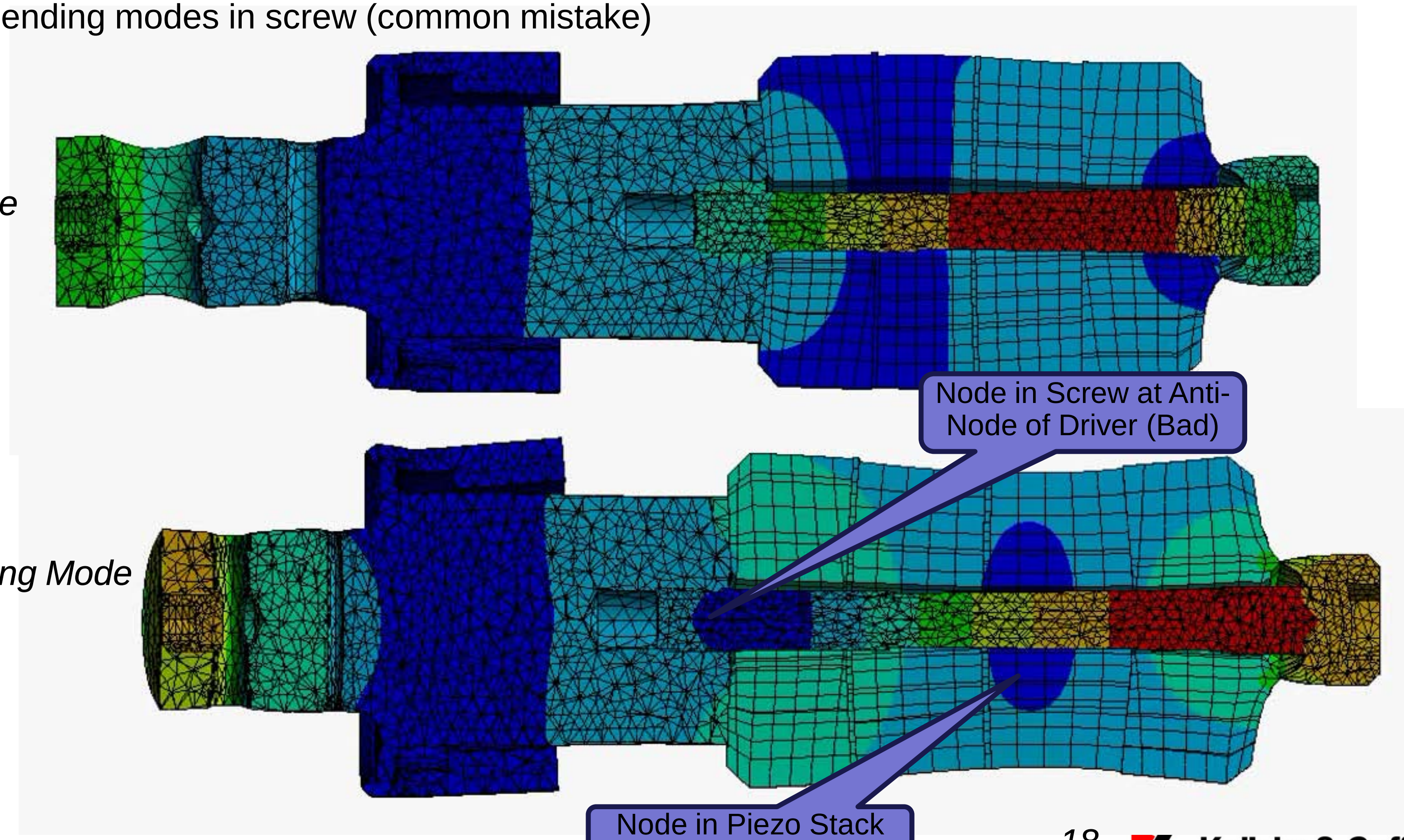

FAILURE MODES OF PRELOAD BOLTS

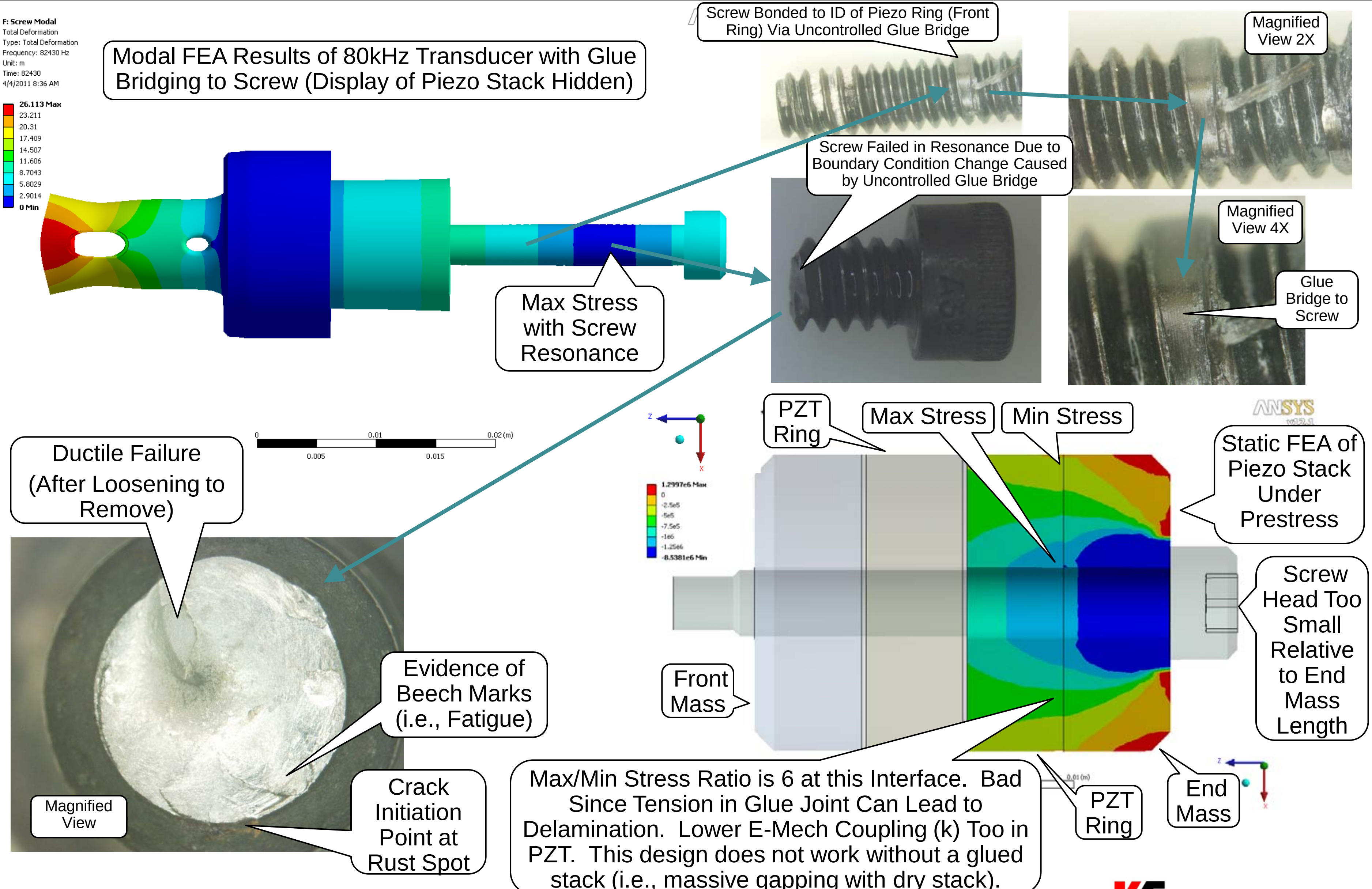

SELECTION OF BOLT MATERIAL

- Optimizing for Strength (Always Use Yield Stress, Not Tensile Strength!)
  - Higher strength materials allow the smallest diameter screw, which maximizes volume of piezo material for a given stack diameter (lower impedance, higher e-mech coupling)
  - Higher strength materials allow for less thread engagement, which minimizes frictional losses (threads can be lossey with higher impedance)
- Optimizing for Transducer Electromechanical Coupling Factor (k)
  - Coupling k is proportional to the transducer "phase window" difference of the antiresonance (fa) and resonance (fr) from Bode plot (i.e. k $\propto$(fa-fr)/fr).
  - The phase window or coupling (k) is maximized when the bolt stiffness is minimized relative to piezo stack (i.e., least amount of stack energy absorbed by preload screw)
  - For example, if preload bolt stiffness is the same as stack stiffness, then (k) will be reduced by at least 50% from the max possible k_{33} for the piezo material
  - The best bolt material is the one with the highest yield strength (σ_y) and the lowest stiffness or elastic modulus (E), i.e., maximize the ratio σ_y /E
    - Highest yield stress material allows the use of the smallest diameter screw (less stiff)
    - Lowest modulus results in the lowest stiffness for a given diameter
    - For example, beryllium copper (BeCu, C17300) screws are better than alloy steel screws for maximizing k (i.e., 160/18.5 = 9 versus 170/30 = 6)
  - Coupling k is maximized when stress in piezo stack is most uniform
    - Custom screws can be advantageous with necking down in unthreaded areas (reduces stiffness) and flared heads for more uniform stress in piezos (especially with end masses that have poor length/diameter (i.e., L/D) ratios in an attempt to maximize piezo volume)
- Wave speed (c=sqrt(E/ρ)) is also a consideration for screw design (phasing, node placement, etc.). Steel, Ti and Al are about the same, where as BeCu is 20% less

SIZING OF PRELOAD BOLTS

- Uniformity of piezo stress is very important when sizing preload bolts

- Nonunifom piezo prestress ultimately results in two simultaneous problems
  - Some volume of the piezo material is insufficiently loaded (i.e., outer diameter of stack) resulting in either tension/delamination in glue joints (for glued stacks) or dynamic gapping at interfaces for dry stacks
  - Some volume of the piezo material will be overloaded (i.e., inner diameter of stack) resulting in severe depoling (i.e., little or no output)

- For example, with near uniform prestress in piezo stack (i.e., max/min stress ratio ≈ 1.0) PZT8 materials can withstand 90 MPa prestress
  - However, with max/min stress ratios in the 1.5-3 range, prestress for PZT8 materials should be reduced to the 30-60 MPa range

- For sizing common alloy steel bolts under static prestress, the catalog recommended seating stress of 120 ksi (e.g. Unbrako) is a good guideline
  - Allows sufficient margin for torquing & dynamic loading up to 170 ksi yield
  - Dynamic loading in bolt typically <10% of prestress levels without resonances
  - Use yield stress, not tensile strength when sizing bolts (yield = preload loss)
  - Can use 150 ksi for more aggressive designs with a compression load fixture

$$\sigma_{seating\,(bolt)} = \frac{\sigma_{piezos} A_{piezos}}{A_{stressed\,(bolt)}} = 120\ ksi$$

PRELOAD BOLT THREAD ENGAGEMENT

Goal: To ensure the length of thread engagement is sufficient to carry the full load necessary to yield the screw without the internal or external threads stripping*

- Tensile Stressed Area of Screw: $A_{ts} = \frac{\pi}{4}\left(D - \frac{0.9743}{n}\right)^2$
- Shear Area of External Thread per Unit Length: $A_{se} = \pi n D_m \left(\frac{1}{2n} + \frac{P_d - D_m}{\sqrt{3}}\right)$
- Shear Area of Internal Thread per Unit Length: $A_{si} = \pi n D_M \left(\frac{1}{2n} + \frac{D_M - D_p}{\sqrt{3}}\right)$

Common design mistake is to use tensile strength for determining minimum thread engagement.

Failure for a transducer must be defined by the yielding of threads where preload is lost.

where D = major diameter, n = number of threads per inch, D_m = max minor diameter of internal thread, D_p = max pitch diameter of internal thread, P_d = min pitch diameter of external thread, and D_M = min major diameter of external thread

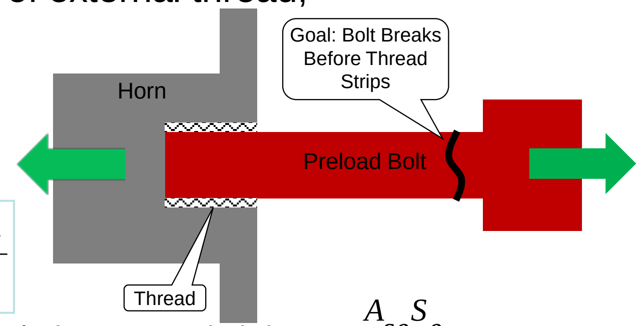

- To Determine Minimum Thread Engagement Length, E_L:
  - A. For same materials for both internal and external threads use: $E_L = \frac{2A_{ts}}{A_{se}}$
  - B. For different materials for internal and external threads, first determine Relative Strength (R), $R = \frac{A_{se}S_e}{A_{si}S_i}$

where S_e = yield strength of external thread material, S_i = yield strength of internal thread material

if $R \le 1$, use the same equation as A: $E_L = \frac{2A_{ts}}{A_{se}}$

if $R > 1$, use: $E_L = \frac{2A_{ts}R}{A_{se}} = \frac{2A_{ts}S_e}{A_{si}S_i}$

*Ref. Walsh or FED-STD-H28/2B

PRELOAD BOLT THREAD ENGAGEMENT

- For example,

with S_e = 170 ksi yield tensile strength for alloy steel screw (class 3A), and S_i = 30 ksi yield tensile strength for annealed 316 stainless steel horn (class 2B), the thread engagement of 8 common UNC screws are:

	D	n	A_{se}	A_{si}	R	A_{ts}	E_L	$E_L(D)$
#2	0.086	56	0.109	0.168	3.683	0.004	0.250	2.9
#4	0.112	40	0.147	0.228	3.659	0.006	0.299	2.7
#6	0.138	32	0.190	0.289	3.724	0.009	0.357	2.6
#8	0.164	32	0.239	0.344	3.924	0.014	0.461	2.8
#10	0.19	24	0.275	0.411	3.788	0.018	0.483	2.5
1/4"	0.25	20	0.383	0.552	3.932	0.032	0.653	2.6
5/16"	0.3125	18	0.489	0.696	3.978	0.052	0.853	2.7
3/8"	0.375	16	0.598	0.845	4.013	0.077	1.040	2.8
							Avg	**2.7**

Tensile strength for annealed 316 stainless is 80 ksi, but yield strength is only 30 ksi. Elongation at failure is a whopping 40%, so if tensile strength is used for the thread engagement length the preload will be long gone before the material can work hardened

Plot of Tensile Stress in Bolt vs Minimum Thread Engagement for:
316 Stainless Steel (annealed), 7075-T6 Aluminum Alloy, and Titanium 6-4 (annealed)

(Class 3A Bolt Threaded in Class 2B Horn)

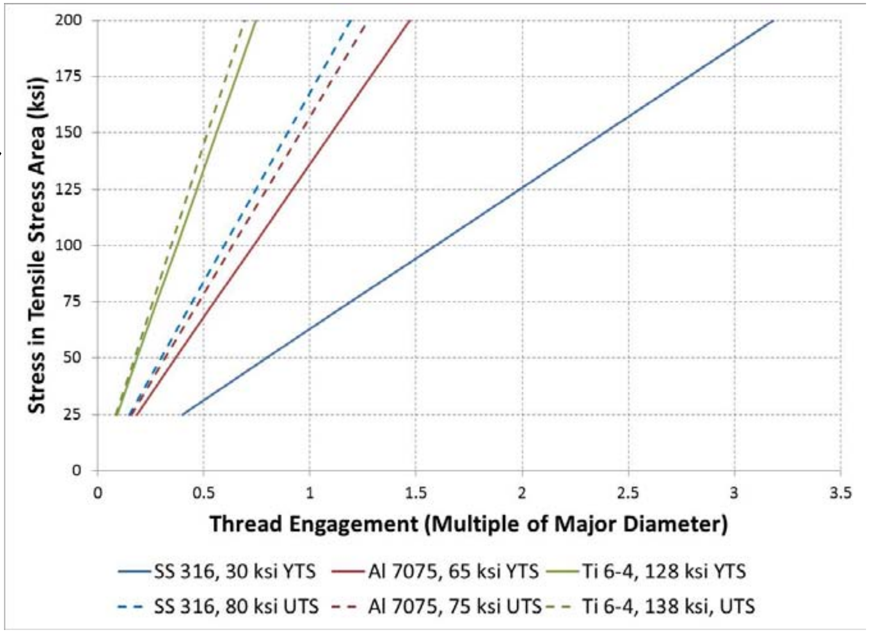

YTS = Yield Stress
UTS = Tensile Strength

PREDICTING PARASITIC BOLT RESONANCES

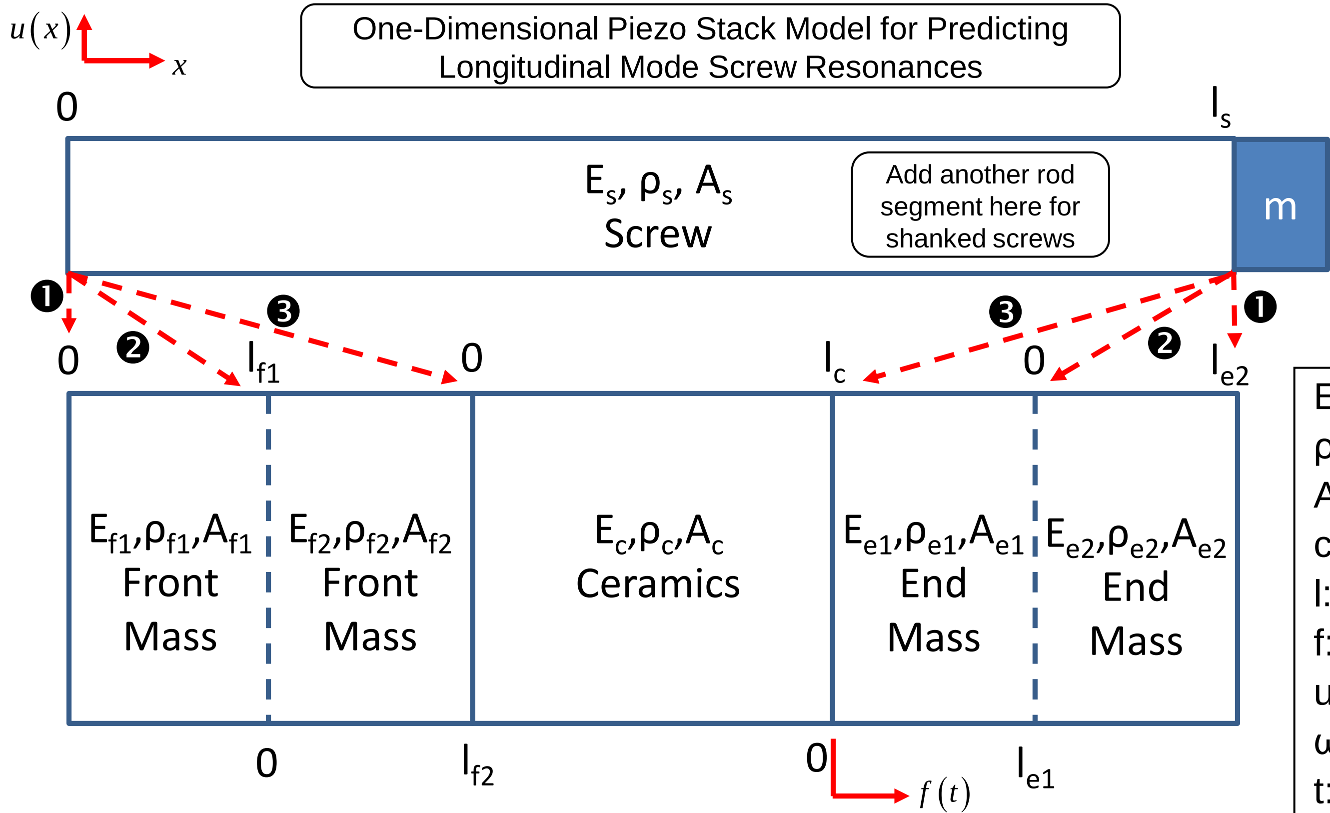

1-D Wave Equation

$$\frac{\partial^2 u}{\partial x^2} = \frac{1}{c^2}\frac{\partial^2 u}{\partial t^2} \qquad f(t) = f_0 \exp(i\omega t)$$

Solution to Forced Response

$$U(x,t) = u(x)\exp(i\omega t) \quad \beta = \frac{\omega}{c} \quad c = \sqrt{\frac{E}{\rho}}$$

$$u(x) = C_1 \sin(\beta x) + C_2 \cos(\beta x)$$

- E: Modulus of Elasticity
- ρ: Mass Density
- A: Area or Thread Pitch Area
- c: Bar Velocity
- l: Length
- f: Force
- u: Displacement
- ω: Angular Frequency
- t: Time m: Mass (Screw head)

Use Short Circuit E_c for Resonance and Open Circuit E_c for Antiresonance

Boundary Conditions (Case ❶, Screw Attached to Ends of Stack)

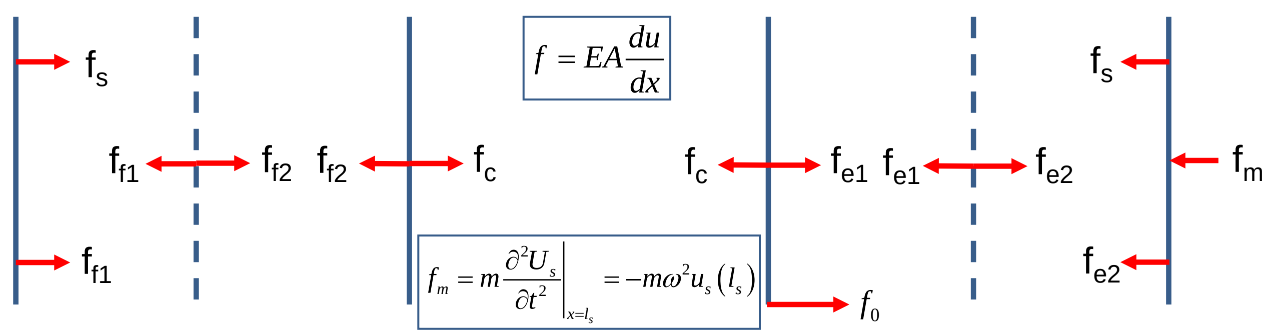

Continuity of Force…&…Displacement

$f_s = -f_{f1}$	$u_s(0) = u_{f1}(0)$
$f_{f1} = f_{f2}$	$u_{f1}(l_{f1}) = u_{f2}(0)$
$f_{f2} = f_c$	$u_{f2}(l_{f2}) = u_c(0)$
$f_0 = f_c - f_{e1}$	$u_c(l_c) = u_{e1}(0)$
$f_{e1} = f_{e2}$	$u_{e1}(l_{e1}) = u_{e2}(0)$
$f_s = -f_{e2} - f_m$	$u_{e2}(l_{e2}) = u_s(0)$

PREDICTING PARASITIC BOLT RESONANCES

Boundary Conditions Assembled in Matrix $Q(\omega)$ for Case ❶ to solve for constants C in Mathcad ($[Q]*[C] = [B]$)

$$Q(\omega) := \begin{pmatrix}
-1 & 0 & 0 & 0 & 0 & 0 & 0 & 0 & 0 & 0 & 1 & 0 \\
0 & 0 & 0 & 0 & 0 & 0 & 0 & 0 & -\cos(\beta_{e2}(\omega)\cdot l_{e2}) & -\sin(\beta_{e2}(\omega)\cdot l_{e2}) & \cos(\beta_s(\omega)\cdot l_s) & \sin(\beta_s(\omega)\cdot l_s) \\
\cos(\beta_{f1}(\omega)\cdot l_{f1}) & \sin(\beta_{f1}(\omega)\cdot l_{f1}) & -1 & 0 & 0 & 0 & 0 & 0 & 0 & 0 & 0 & 0 \\
0 & 0 & \cos(\beta_{f2}(\omega)\cdot l_{f2}) & \sin(\beta_{f2}(\omega)\cdot l_{f2}) & -1 & 0 & 0 & 0 & 0 & 0 & 0 & 0 \\
0 & 0 & 0 & 0 & \cos(\beta_c(\omega)\cdot l_c) & \sin(\beta_c(\omega)\cdot l_c) & -1 & 0 & 0 & 0 & 0 & 0 \\
0 & 0 & 0 & 0 & 0 & 0 & \cos(\beta_{e1}(\omega)\cdot l_{e1}) & \sin(\beta_{e1}(\omega)\cdot l_{e1}) & -1 & 0 & 0 & 0 \\
0 & E_{f1}\cdot A_{f1}\cdot\beta_{f1}(\omega) & 0 & 0 & 0 & 0 & 0 & 0 & 0 & 0 & 0 & E_s\cdot A_s\cdot\beta_s(\omega) \\
0 & 0 & 0 & 0 & -E_c\cdot A_c\cdot\beta_c(\omega)\cdot\sin(\beta_c(\omega)\cdot l_c) & E_c\cdot A_c\cdot\beta_c(\omega)\cdot\cos(\beta_c(\omega)\cdot l_c) & 0 & -E_{e1}\cdot A_{e1}\cdot\beta_{e1}(\omega) & 0 & 0 & 0 & 0 \\
0 & 0 & 0 & 0 & 0 & 0 & 0 & 0 & -E_{e2}\cdot A_{e2}\cdot\beta_{e2}(\omega)\cdot\sin(\beta_{e2}(\omega)\cdot l_{e2}) & E_{e2}\cdot A_{e2}\cdot\beta_{e2}(\omega)\cdot\cos(\beta_{e2}(\omega)\cdot l_{e2}) & M1(\omega) & M2(\omega) \\
-E_{f1}\cdot A_{f1}\cdot\beta_{f1}(\omega)\cdot\sin(\beta_{f1}(\omega)\cdot l_{f1}) & E_{f1}\cdot A_{f1}\cdot\beta_{f1}(\omega)\cdot\cos(\beta_{f1}(\omega)\cdot l_{f1}) & 0 & -E_{f2}\cdot A_{f2}\cdot\beta_{f2}(\omega) & 0 & 0 & 0 & 0 & 0 & 0 & 0 & 0 \\
0 & 0 & -E_{f2}\cdot A_{f2}\cdot\beta_{f2}(\omega)\cdot\sin(\beta_{f2}(\omega)\cdot l_{f2}) & E_{f2}\cdot A_{f2}\cdot\beta_{f2}(\omega)\cdot\cos(\beta_{f2}(\omega)\cdot l_{f2}) & 0 & -E_c\cdot A_c\cdot\beta_c(\omega) & 0 & 0 & 0 & 0 & 0 & 0 \\
0 & 0 & 0 & 0 & 0 & 0 & -E_{e1}\cdot A_{e1}\cdot\beta_{e1}(\omega)\cdot\sin(\beta_{e1}(\omega)\cdot l_{e1}) & E_{e1}\cdot A_{e1}\cdot\beta_{e1}(\omega)\cdot\cos(\beta_{e1}(\omega)\cdot l_{e1}) & 0 & -E_{e2}\cdot A_{e2}\cdot\beta_{e2}(\omega) & 0 & 0
\end{pmatrix}$$

Forcing Function Matrix

$$B(f_0) := \begin{pmatrix} 0 \\ 0 \\ 0 \\ 0 \\ 0 \\ 0 \\ 0 \\ f_0 \\ 0 \\ 0 \\ 0 \\ 0 \end{pmatrix}$$

Invert Q to Solve for C

$$C(\omega, f_0) := Q(\omega)^{-1}\cdot B(f_0)$$

$$M1(\omega) := -E_s\cdot A_s\cdot\beta_s(\omega)\cdot\sin(\beta_s(\omega)\cdot l_s) - m\cdot\omega^2\cdot\cos(\beta_s(\omega)\cdot l_s)$$

$$M2(\omega) := E_s\cdot A_s\cdot\beta_s(\omega)\cdot\cos(\beta_s(\omega)\cdot l_s) - m\cdot\omega^2\cdot\sin(\beta_s(\omega)\cdot l_s)$$

Assemble Equations for Displacement Mode Shapes Using Constants

$$u_{f1}(x, \omega, f_0) := C(\omega, f_0)_1\cdot\cos(\beta_{f1}(\omega)\cdot x) + C(\omega, f_0)_2\cdot\sin(\beta_{f1}(\omega)\cdot x)$$

$$u_{f2}(x, \omega, f_0) := C(\omega, f_0)_3\cdot\cos(\beta_{f2}(\omega)\cdot x) + C(\omega, f_0)_4\cdot\sin(\beta_{f2}(\omega)\cdot x)$$

$$u_c(x, \omega, f_0) := C(\omega, f_0)_5\cdot\cos(\beta_c(\omega)\cdot x) + C(\omega, f_0)_6\cdot\sin(\beta_c(\omega)\cdot x)$$

$$u_{e1}(x, \omega, f_0) := C(\omega, f_0)_7\cdot\cos(\beta_{e1}(\omega)\cdot x) + C(\omega, f_0)_8\cdot\sin(\beta_{e1}(\omega)\cdot x)$$

$$u_{e2}(x, \omega, f_0) := C(\omega, f_0)_9\cdot\cos(\beta_{e2}(\omega)\cdot x) + C(\omega, f_0)_{10}\cdot\sin(\beta_{e2}(\omega)\cdot x)$$

$$u_s(x, \omega, f_0) := C(\omega, f_0)_{11}\cdot\cos(\beta_s(\omega)\cdot x) + C(\omega, f_0)_{12}\cdot\sin(\beta_s(\omega)\cdot x)$$

Compute Transfer Functions Versus Frequency

$$T_{f1}(\omega) := \frac{u_{f1}(0, \omega, f_0)}{f_0} \qquad T_c(\omega) := \frac{u_c(0, \omega, f_0)}{f_0} \qquad T_{e1}(\omega) := \frac{u_{e1}(0, \omega, f_0)}{f_0}$$

$$T_{f2}(\omega) := \frac{u_{f2}(0, \omega, f_0)}{f_0} \qquad T_s(\omega) := \frac{u_s(l_s, \omega, f_0)}{f_0} \qquad T_{e2}(\omega) := \frac{u_{e2}(0, \omega, f_0)}{f_0}$$

For Spring-Mass Boundary Condition

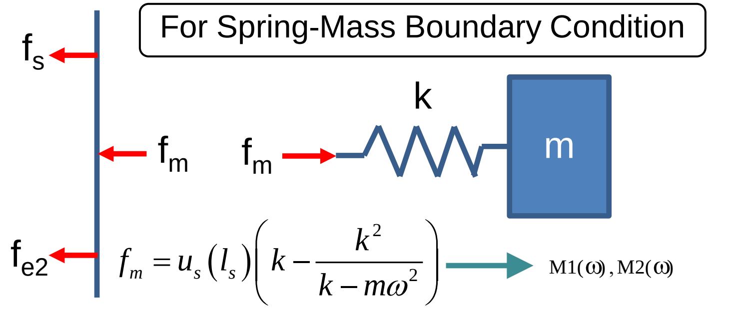

$$f_m = u_s(l_s)\left(k - \frac{k^2}{k - m\omega^2}\right)$$

PREDICTING PARASITIC BOLT RESONANCES

40kHz Half Wave Langevin Stack Example

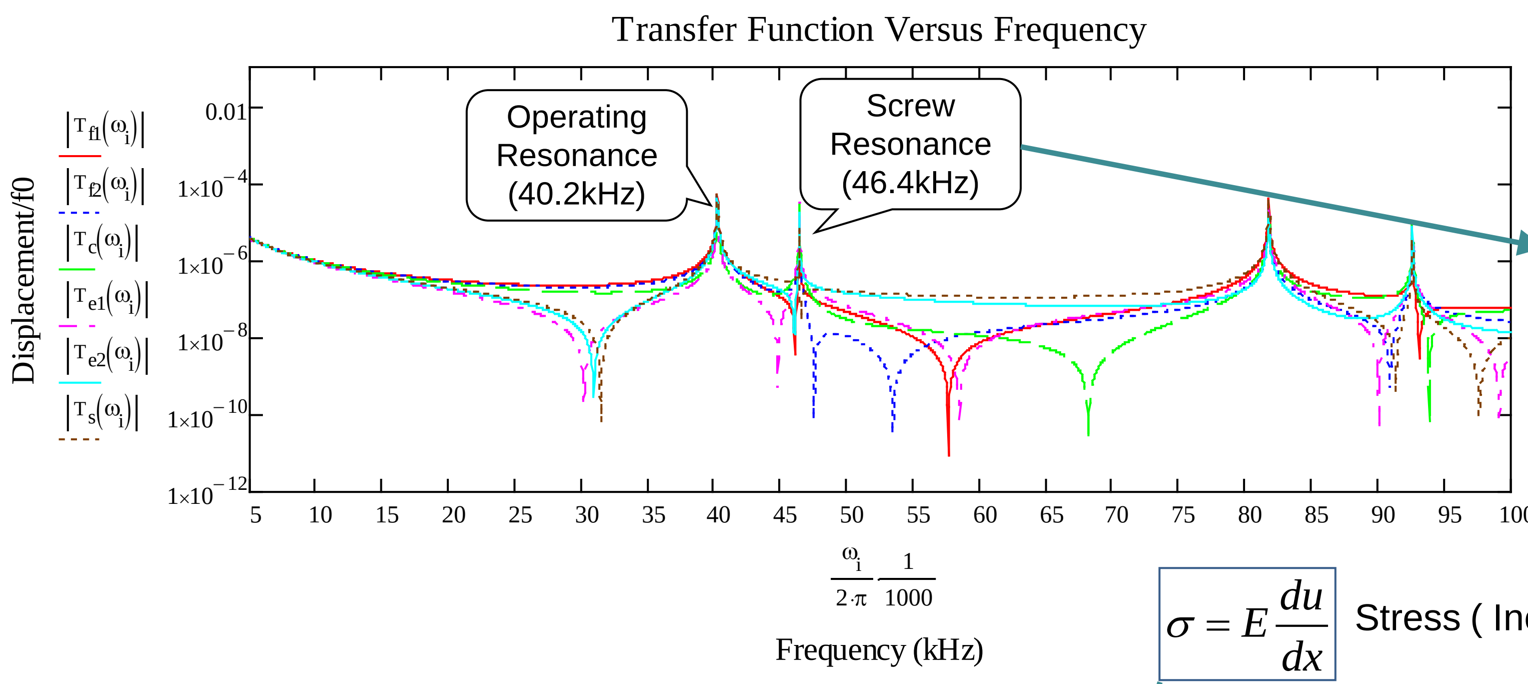

Good guideline is >10% frequency separation for dry stacks and >20% frequency separation for glued stacks

$$\sigma = E\frac{du}{dx}$$

Stress (Increases with Slope)

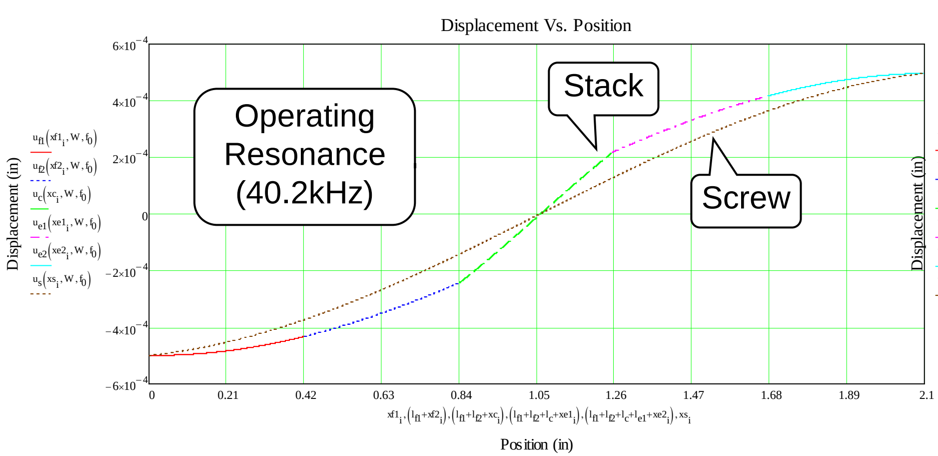

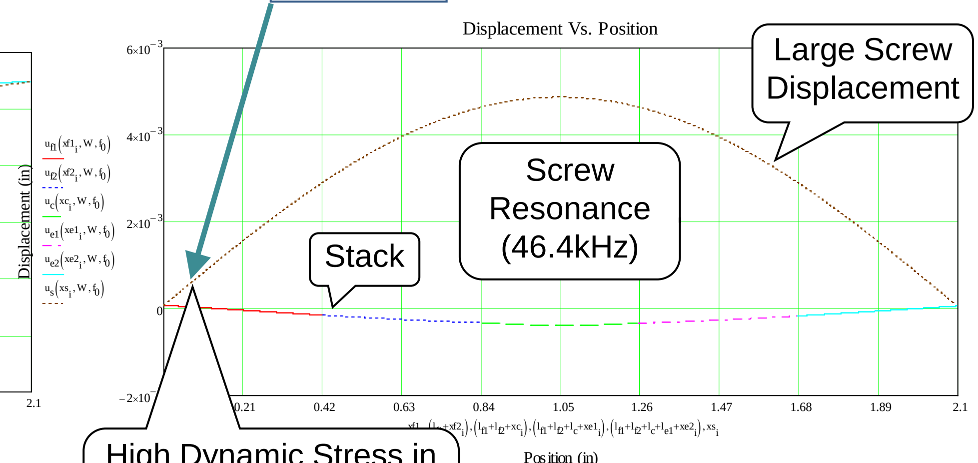

High Dynamic Stress in Screw. Failure Eminent Due to Yielding

PREDICTING PARASITIC BOLT RESONANCES

One-Dimensional Model for Predicting Bending Mode Screw Resonances

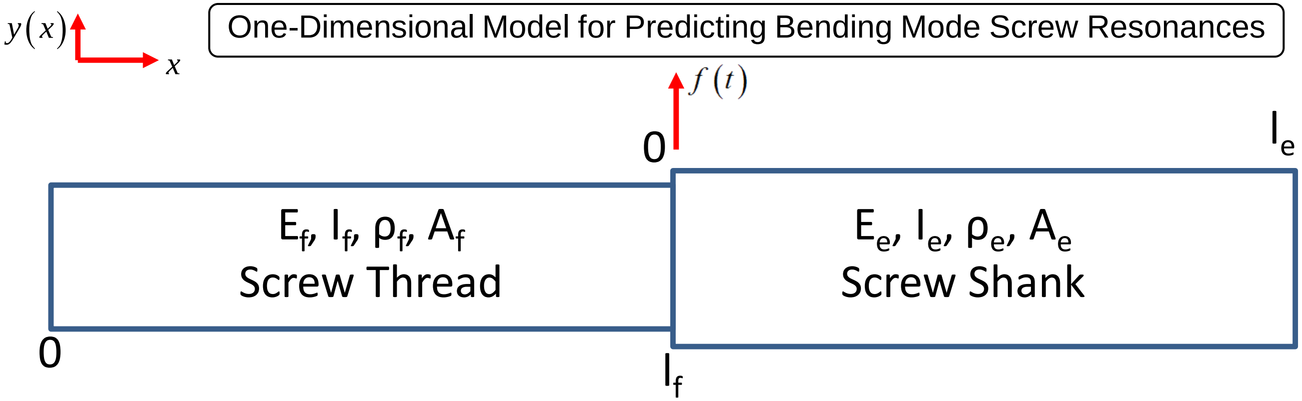

1-D Flexural Wave Equation

$$\frac{\partial^4 y}{\partial x^4} = \frac{1}{c^2}\frac{\partial^2 u}{\partial t^2} \qquad f(t) = f_0 \exp(i\omega t)$$

Assume Solution

$$Y(x,t) = y(x)\exp(i\omega t) \quad a = \sqrt{\frac{EI}{\rho A}} \quad \beta = \frac{\omega}{a}$$

Solution to Forced Response $y(x) = C_1 \sin(\beta x) + C_2 \cos(\beta x) + C_3 \sinh(\beta x) + C_4 \cosh(\beta x)$

Common Boundary Conditions (❶ & ❷)

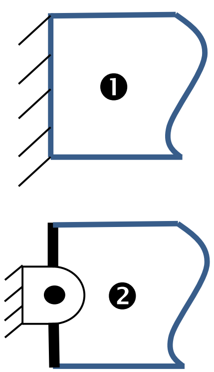

$y_f(0) = 0$	Displacement	$y_e(l_e) = 0$
$\left.\frac{dy_f}{dx}\right\|_{x=0} = 0$	Slope	$\left.\frac{dy_e}{dx}\right\|_{x=l_e} = 0$
$y_f(0) = 0$	Displacement	$y_e(l_e) = 0$
$\left.\frac{d^2y_f}{dx^2}\right\|_{x=0} = 0$	Moment	$\left.\frac{d^2y_e}{dx^2}\right\|_{x=l_e} = 0$

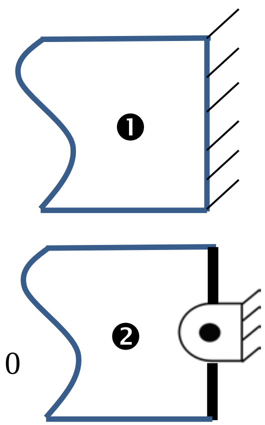

E: Modulus of Elasticity
ρ: Mass Density
A: Area or Thread Pitch Area
I: Inertia
a: Beam Constant
l: Length
V: Shear
M: Moment
y: Displacement
ω: Angular Frequency
t: Time

Slope Continuity

$$\left.\frac{dy_f}{dx}\right|_{x=l_f} = \left.\frac{dy_e}{dx}\right|_{x=0}$$

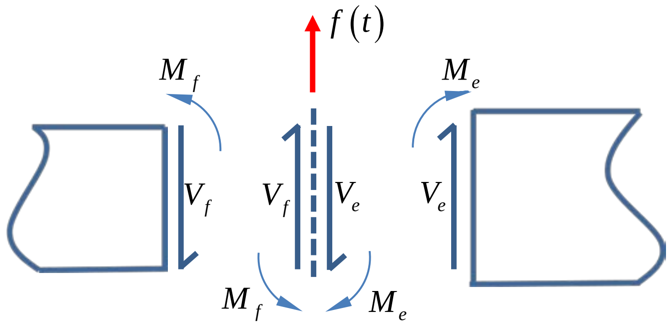

Shear Force Continuity

$$f_0 = V_e - V_f$$

$$f_0 = E_e I_e \left.\frac{d^3 y_e}{dx^3}\right|_{x=0} - E_f I_f \left.\frac{d^3 y_f}{dx^3}\right|_{x=l_f}$$

Moment Continuity

$$M_f = M_e$$

$$E_f I_f \left.\frac{d^2 y_f}{dx^2}\right|_{x=l_f} = E_e I_e \left.\frac{d^2 y_e}{dx^2}\right|_{x=0}$$

PREDICTING PARASITIC BOLT RESONANCES

Boundary Conditions Assembled in Matrix $Q(\omega)$ for Case ❶ to solve for constants C in Mathcad ($[Q]*[C] = [B]$)

$$Q(\omega) := \begin{pmatrix} 0 & 1 & 0 & 1 & 0 & 0 & 0 & 0 \\ \sin(\beta_f(\omega)\cdot l_f) & \cos(\beta_f(\omega)\cdot l_f) & \sinh(\beta_f(\omega)\cdot l_f) & \cosh(\beta_f(\omega)\cdot l_f) & 0 & -1 & 0 & -1 \\ 0 & 0 & 0 & 0 & \sin(\beta_e(\omega)\cdot l_e) & \cos(\beta_e(\omega)\cdot l_e) & \sinh(\beta_e(\omega)\cdot l_e) & \cosh(\beta_e(\omega)\cdot l_e) \\ \beta_f(\omega) & 0 & \beta_f(\omega) & 0 & 0 & 0 & 0 & 0 \\ 0 & 0 & 0 & 0 & \beta_e(\omega)\cos(\beta_e(\omega)\cdot l_e) & -\beta_e(\omega)\sin(\beta_e(\omega)\cdot l_e) & \beta_e(\omega)\cosh(\beta_e(\omega)\cdot l_e) & \beta_e(\omega)\sinh(\beta_e(\omega)\cdot l_e) \\ \beta_f(\omega)\cos(\beta_f(\omega)\cdot l_f) & -\beta_f(\omega)\sin(\beta_f(\omega)\cdot l_f) & \beta_f(\omega)\cosh(\beta_f(\omega)\cdot l_f) & \beta_f(\omega)\sinh(\beta_f(\omega)\cdot l_f) & -\beta_e(\omega) & 0 & -\beta_e(\omega) & 0 \\ E_f\cdot I_f\cdot \beta_f(\omega)^3\cdot\cos(\beta_f(\omega)\cdot l_f) & -E_f\cdot I_f\cdot \beta_f(\omega)^3\cdot\sin(\beta_f(\omega)\cdot l_f) & -E_f\cdot I_f\cdot \beta_f(\omega)^3\cdot\cosh(\beta_f(\omega)\cdot l_f) & -E_f\cdot I_f\cdot \beta_f(\omega)^3\cdot\sinh(\beta_f(\omega)\cdot l_f) & -E_e\cdot I_e\cdot \beta_e(\omega)^3 & 0 & E_e\cdot I_e\cdot \beta_e(\omega)^3 & 0 \\ -E_f\cdot I_f\cdot \beta_f(\omega)^2\cdot\sin(\beta_f(\omega)\cdot l_f) & -E_f\cdot I_f\cdot \beta_f(\omega)^2\cdot\cos(\beta_f(\omega)\cdot l_f) & E_f\cdot I_f\cdot \beta_f(\omega)^2\cdot\sinh(\beta_f(\omega)\cdot l_f) & E_f\cdot I_f\cdot \beta_f(\omega)^2\cdot\cosh(\beta_f(\omega)\cdot l_f) & 0 & E_e\cdot I_e\cdot \beta_e(\omega)^2 & 0 & -E_e\cdot I_e\cdot \beta_e(\omega)^2 \end{pmatrix}$$

Invert Q to Solve for C

$$C(\omega, f_0) := Q(\omega)^{-1}\cdot B(f_0)$$

Forcing Function Matrix

$$b(f_0) := \begin{pmatrix} 0 \\ 0 \\ 0 \\ 0 \\ 0 \\ 0 \\ f_0 \\ 0 \end{pmatrix}$$

Assemble Equations for Displacement Mode Shapes Using Constants

$$y_f(x,\omega,f_0) := c(\omega,f_0)_1\cdot\sin(\beta_f(\omega)\cdot x) + c(\omega,f_0)_2\cdot\cos(\beta_f(\omega)\cdot x) + c(\omega,f_0)_3\cdot\sinh(\beta_f(\omega)\, x) + c(\omega,f_0)_4\cdot\cosh(\beta_f(\omega)\cdot x)$$

$$y_e(x,\omega,f_0) := c(\omega,f_0)_5\cdot\sin(\beta_e(\omega)\cdot x) + c(\omega,f_0)_6\cdot\cos(\beta_e(\omega)\cdot x) + c(\omega,f_0)_7\cdot\sinh(\beta_e(\omega)\, x) + c(\omega,f_0)_8\cdot\cosh(\beta_e(\omega)\cdot x)$$

Compute Transfer Functions Versus Frequency

$$T_f(\omega) := \frac{y_f(l_f,\omega,f_0)}{f_0} \qquad T_e(\omega) := \frac{y_e(0,\omega,f_0)}{f_0}$$

Warning!: Solution above ignores shear deformations and rotary inertia effects making it less accurate for higher order modes. See Graff reference for solution to equations below to include these effects:

$$GA\kappa\left(\frac{\partial\varphi}{\partial x}-\frac{\partial^2 y}{\partial x^2}\right)+\rho A\frac{\partial^2 y}{dt^2}=q(x,t), \quad GA\kappa\left(\frac{\partial y}{\partial x}-\varphi\right)+EI\frac{\partial^2\varphi}{dx^2}=\rho I\frac{\partial^2\varphi}{dt^2}$$

PREDICTING PARASITIC BOLT RESONANCES

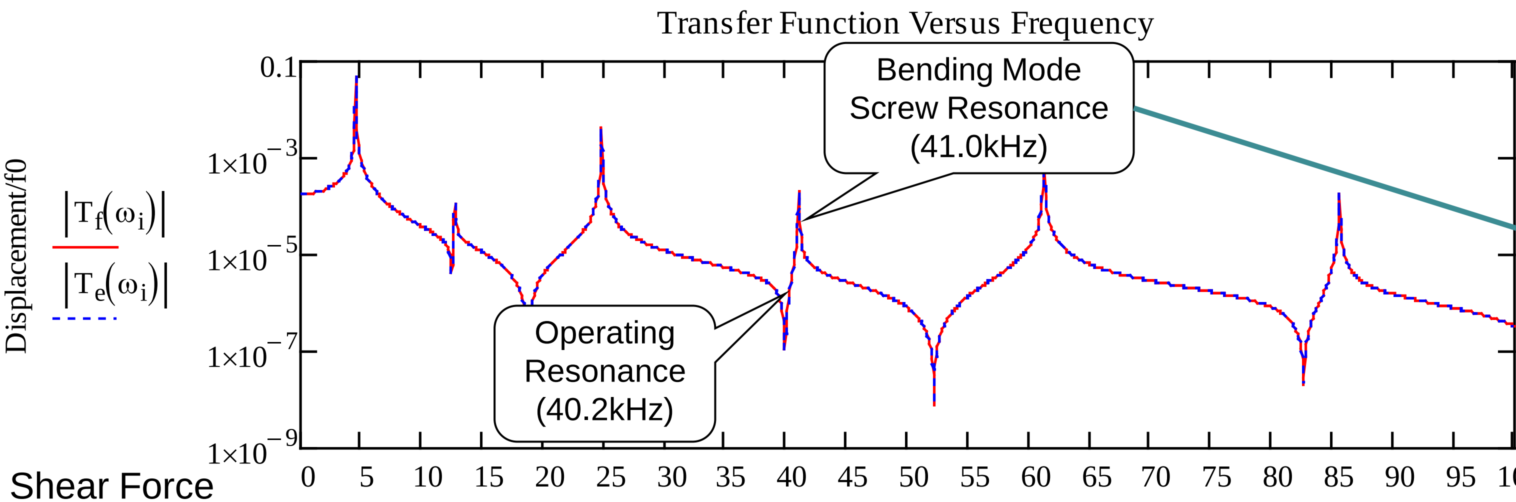

40kHz Half Wave Langevin Stack Example

Good guideline is >10% frequency separation for dry stacks and >20% frequency separation for glued stacks

$$\frac{\omega_i}{2\cdot\pi}\cdot\frac{1}{1000}$$

Frequency (kHz)

Shear Force

$$V_f(x,\omega,f_0) := -E_f\cdot I_f\cdot\frac{d^3}{dx^3}y_f(x,\omega,f_0) \qquad V_e(x,\omega,f_0) := -E_e\cdot I_e\cdot\frac{d^3}{dx^3}y_e(x,\omega,f_0)$$

Moment

$$M_f(x,\omega,f_0) := -E_f\cdot I_f\cdot\frac{d^2}{dx^2}y_f(x,\omega,f_0) \qquad M_e(x,\omega,f_0) := -E_e\cdot I_e\cdot\frac{d^2}{dx^2}y_e(x,\omega,f_0)$$

Stress

$$\sigma_f(x,\omega,f_0) := M_f(x,\omega,f_0)\cdot\frac{d_f}{2\cdot I_f} \qquad \sigma_e(x,\omega,f_0) := M_e(x,\omega,f_0)\cdot\frac{d_e}{2\cdot I_e}$$

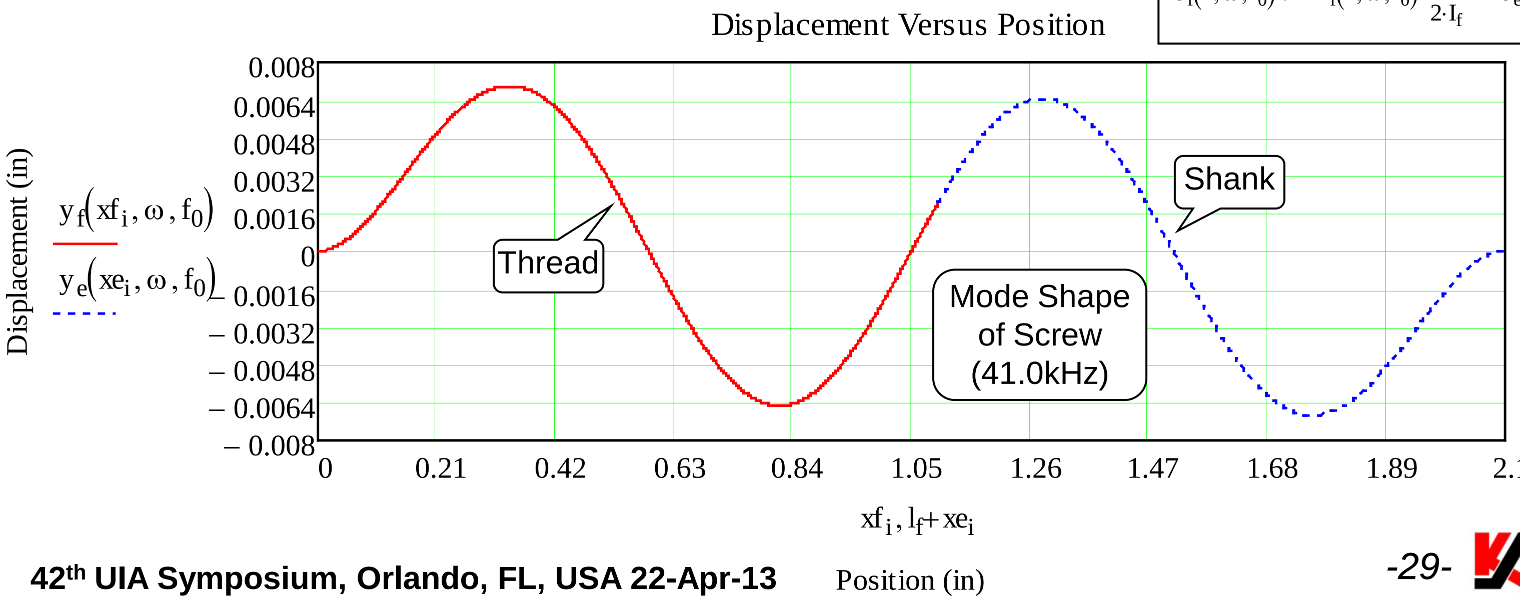

PREDICTING PARASITIC BOLT RESONANCES

❖ Comparison of 1-D 40kHz Langevin Solution to FEA Model

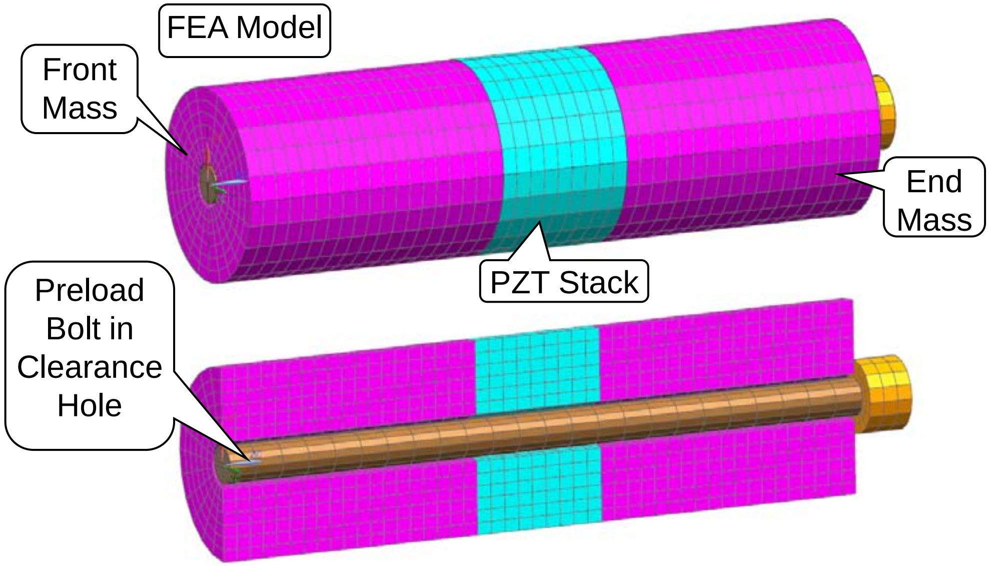

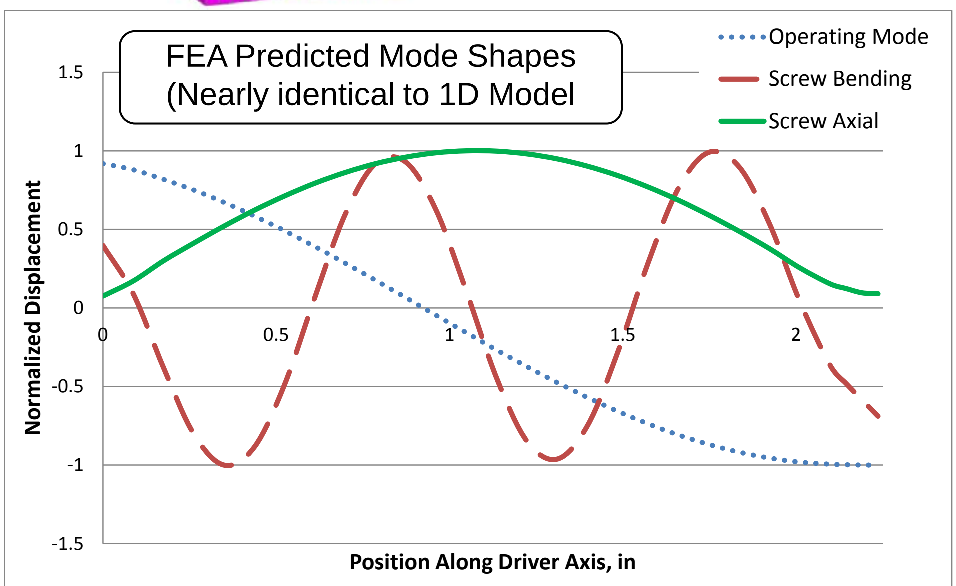

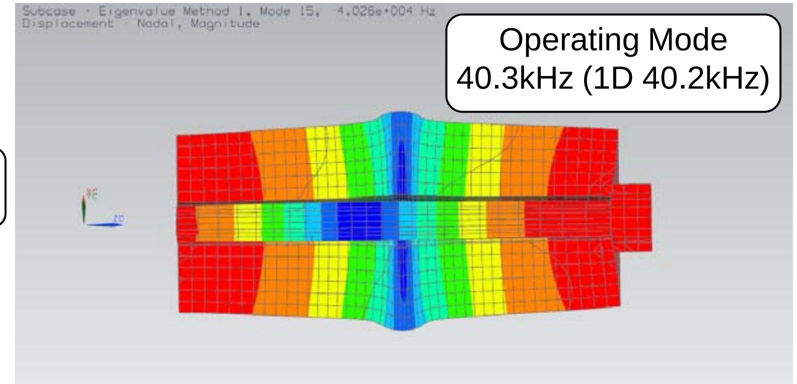

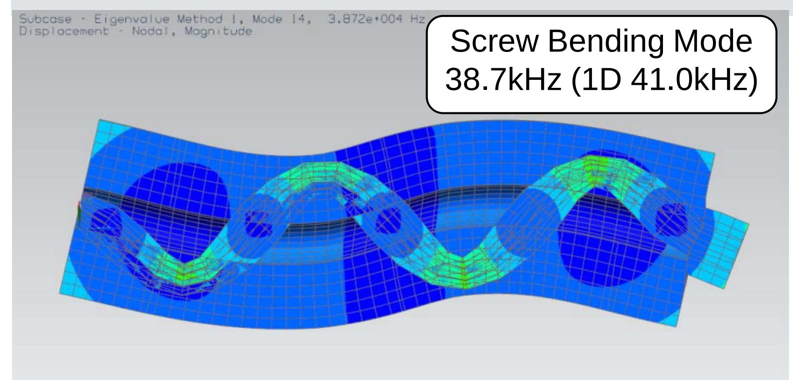

CONCLUSIONS

- The preload screw configuration and design requires a detailed trade-off analysis
  - Need to optimize stress uniformity, e-mech coupling and stack symmetry, while minimizing interaction of parasitic screw modes
- Screw resonances can manifest as both longitudinal and bending modes
  - Actual boundary conditions can be tricky to model in FEA making prediction difficult
  - Commonly used axis-symmetric FEA models can not predict screw bending modes
  - Screw boundary conditions can especially vary with glued piezo stack designs, so greater separation with parasitic screw modes is required compared to dry stacks
  - Uncontrolled screw resonances often lead to preload loss and screw failure, but at the very least they can negatively effect transducer performance
- The best bolt material is the one with the highest yield strength (σ_y) and the lowest stiffness or elastic modulus (E), i.e., maximize the ratio σ_y / E
  - The phase window or coupling (k) is maximized when the bolt stiffness is minimized relative to piezo stack
- The sizing of preload screws and determination of minimum thread engagement should always be done based on yield strength (yielding = preload loss)
  - Adequate thread engagement length based on yield stress is critical for both the preload screw and internal threads of horn to prevent preload loss under dynamics
  - Uniformity of prestress effects both bolt sizing and e-mech coupling
- Simple 1-D wave equation models can be a fast and effective way to identify locations of parasitic screw resonance for many piezo stack configurations
  - Use 10% frequency separation for dry stacks and 20% for glued stacks

REFERENCES

- K. F. Graff, Wave Motion in Elastic Solids. New York, NY: Dover Publications, 1991.
- R. S. Woollett, “Transducer Comparison Methods Based on the Electromechanical Coupling-Coefficient Concept,” 1957 IRE National Convention, p. 23-27, IEEE Xplore.
- R. A. Walsh, Electromechanical Design Handbook. Blue Ridge Summit, PA: TAB Books, 1990.

REFERENCES CON'T

- D. Stansfield, Underwater Electroacoustic Transducers. Los Altos, CA: Peninsula Publishing, 1991.
- O. B. Wilson, Introduction to Theory and Design of Sonar Transducers. Los Altos, CA: Peninsula Publishing, 1991.
- C. H. Sherman and J. L. Butler, Transducers and Arrays for Underwater Sound. New York, NY: Springer Science, 2007.
- K. Uchino and J. R. Giniewicz, Micromechatronics. New York, NY: Marcel Dekker, 2003.
- K. Uchino, Ferroelectric Devices. New York, NY: Marcel Dekker, 2010.
- D. A. DeAngelis and G. W. Schulze, "The Effects of Piezoelectric Ceramic Dissipation Factor on the Performance of Ultrasonic Transducers," 2012 UIA Symposium Proceedings, American Institute of Physics.
- D. A. DeAngelis and G. W. Schulze, "Advanced Bode Plot Techniques for Ultrasonic Transducers," 2011 UIA Symposium Proceedings, American Institute of Physics.
- D. A. DeAngelis and G. W. Schulze, "Optimizing Piezoelectric Ceramic Thickness in Ultrasonic Transducers," 2010 UIA Symposium Proceedings, IEEE XPlore.
- D. A. DeAngelis and G. W. Schulze, "Optimizing Piezoelectric Crystal Preload in Ultrasonic Transducers," 2009 UIA Symposium Proceedings, IEEE XPlore.
- D. A. DeAngelis and D. C. Schalcosky, "The Effect of PZT8 Piezoelectric Crystal Aging on Mechanical and Electrical Resonances in Ultrasonic Transducers," 2006 IEEE Ultrasonics Symposium, Session P2O-10.

QUESTIONS?